Dysfunctional Glucose Metabolism and Progression of Alzheimer's disease.

By

Mawara Farooq Awan

Reg no: 00000276521

MS Biomedical Sciences

Dr. Saima Zafar

(SMME)

National University of Sciences and Technology (NUST) Islamabad,

Pakistan 2020

A thesis submitted in partial fulfillment of the requirement for the degree of Master of Science in Biomedical Sciences

By

Mawara Farooq Awan 00000276521

Supervised by Dr. Saima Zafar

School of Mechanical and Manufacturing Engineering (SMME)

National University of Sciences and Technology (NUST) Islamabad,

Pakistan 2021.

THESIS ACCEPTANCE CERTIFICATE

Certified that final contents and form of MS/MPhil thesis entitled **"Dysfunctional Glucose Metabolism and Progression Of Alzheimer" written by Mawara Farooq Awan, (Registration No. 00000276521)**, of SMME, has been vetted by undersigned, found complete in all respects as per NUST Status/Regulations, is free of plagiarism, errors, and mistakes and is accepted as partial fulfillment for the award of MS/MPhil degree. It is further certified that necessary amendments as pointed out by GEC members of the scholar have also been incorporated in the said thesis.

Signature:

Supervisor: **Dr. Saima zafar**

Date:

Signature (HoD):

Date:

Countersign by

Signature (Dean/Principal):

Date:

CERTIFICATE FOR PLAGIARISM

It is to confirm that the MS thesis entitled **"Dysfunctional Glucose Metabolism and Progression of Alzheimer's disease"** by Ms. Mawara Farooq Awan, Registration No. 00000276521 has been examined by me. I undertake

that,

1.Thesis has significant new work/knowledge as compared to already elsewhere. No sentence, table, equation, diagram, paragraph, or section has been copied verbatim from previous work except when placed under quotation marks and duly referenced.

2.The work presented is original and own work if the author i.e. there is no plagiarism. No idea, results, or words of others have been presented as the author's work.

3.There is no fabrication of data or results such that the research is not accurately represented in the records. The thesis has been checked using Turnitin (a copy of the originality report attached and found within the limits as per HEC plagiarism policy and instruction issued from time to time).

(Supervisor)

Dr. Saima Zafar

Associate Professor

Biomedical Sciences, SMME NUST

DECLARATION

I, Mawara Farooq Awan, declare that all work presented in this thesis is the result of my work. Where information has been derived from other sources, I confirm that this has been mentioned in the thesis. The work herein was carried out while I was a post-graduate student at the School of Mechanical and Manufacturing Engineering (SMME), NUST under the supervision of Dr. Saima Zafar.

Mawara Farooq

00000276521

Dedicated to

My Beloved Parents

For their endless support, endearment, care & encouragement

My Supervisor

For her guidance and patience

My Friends

For standing with me in every high and low

Acknowledgments

To start with the greatest name of Allah, the Most Gracious & the Most Merciful I would express my heartfelt thanks to my exalted supervisor, **Dr. Saima Zafar** for her insightful advice, patience, motivation, care, and support throughout my research work. Her constant interest and guidance enabled me to attain my research objectives with ease. She believed in me and provided me every opportunity to excel for which I am very thankful to her. My special regards to my thesis committee members; **Dr. Nosheen Fatima, Dr. Rumeza Hanif**, and **Dr. Omer Gillani** for their valuable suggestions. I would also like to extend my thankfulness to Principal SMME, **Dr. Javaid Iqbal** for providing necessary research facilities in the department and aspiring me. At last, I would like to thank the whole faculty of Biomedical Sciences for their support and love.

I owe this thesis to my parents ***Umer Farooq*** and ***Tahira Malik*** without whom I am nothing. And a special thanks to a very special person in my life, ***Bilawal Arsal*** Whatever I am today, it is due to my family. My sincere thanks go to all the Seniors I encountered here at SMME. I would like to thank my friends ***Tayyaba Shafique Khan, Maria Zeb, Shehzadi Erum Fatima, Nimra Mehmood Malik*** for making my time at NUST a memorable one, reaching me out first in every difficulty, and were there for me throughout my academic years at NUST.

Mawara Farooq

Table of Content

List of Table

List of Figures

ABSTRACT:

Alzheimer's disease (AD) is the degenerative brain disorder, which is the most common form of dementia resulting in progressive memory loss, impaired thinking and brain degeneration.In cerebral cortex the neurons degenerated and demonstrated the emergence of neurofibrillary tangles and plaques containing β amyloids. Glucose is an essential energy substrate to sustain neuronal activity and is taken up via glucose transporters expressed in the brain endothelium, astrocytes and neurons.Emerging evidence suggests that impaired cerebral glucose metabolism, deposition of Aβ aggregates, oxidative damage, results in thinning of key brain areas, which is invariant pathological feature of AD. The main objective of this study was to find interactive association between glucose metabolism and AD progression.Furthermore identification of differentially regulated proteins involved in glucose metabolic pathway and to further characterize the therapeutic intervention towards AD progression.In this study we found eight dysregulated glucose linked proteins with AD.

CHAPTER 1: INTRODUCTION

The most common reason of dementia is Alzheimer's disease (AD). It is the world's most prevalent neurodegenerative illness (Jellinger, 2020). The amyloid-beta and tau aggregates in the brain were frequently surrounded by intraneuronal neurofibrillary tangles (Mayeux and Stern, 2012).It is considered as slow onset and perceptive dysfunction in memory, response, and language, as well as impairment in daily life functions (Jellinger, 2020). Alzheimer's disease causes impairments in visuospatial perception, navigation, decision-making, and language disruption. Cognitive destruction affects the behavioral and psychological signs of dementia. These cognitive deficits have an impact on everyday tasks as well as numerous behavioral and psychological dementia symptoms. Amyloidosis, swelling, neuron degeneration, and the emergence of behavioral and psychiatric symptoms are all molecular and clinical processes that occur in Alzheimer's disease (Huang et al., 2020).

AD affected 10% of persons above age of 65, it doubles in frequency every 5 years until they reach the age of 80, at which point it affects more than 40% of people. Alzheimer's disease is primarily caused by old age. When people with normal minds get Alzheimer's disease, their thinking patterns shift unexpectedly. These symptoms worsen between the preclinical and early stages of Alzheimer's disease (Mosconi, 2013). Genetic subtypes of this disease manifest themselves medically at 45 age (Shafiq, 2019). Alzheimer's disease patients with genetic subtypes make up 5% of the total. According to the 2015 World Alzheimer Report , there were 46.8 million individuals were existing with dementia.Entire worldwide socioeconomic dementia rate is projected was $818 billion USD.It accounts for 60–70% of dementia cases (AD) (Huang et al., 2020).

The most severe characteristic of disease is beta-amyloid and tangles of neurofibrillary, which generate tau aggregates, lesions, synaptic loss, and vascular amyloid deposits. These pathogenic targets were utilized in clinical trials to test treatment options (Tang et al., 2019). Total perception deficiencies characterize Alzheimer's disease. It starts with memory loss and progresses to decreased decision-making and perceptual ability (Mosconi, 2005). Slow intellectual drop in the first stage progresses to a spot when it varies, resulting in an abrupt loss of cognitive abilities, which is a representative of clinical type of this disease. Pathologies of Alzheimer's disease include response microgliosis, neuronal loss, matter in white, and junction between two nerve cells. The etiological process behind these neurological changes in AD are not clear, but they are influenced by genetic and environmental features. The etiological mechanisms of AD are influenced by both genetic and environmental factors, but neuropathological changes in AD are not well understood (Reitz et al., 2011). When intellectual abilities suddenly deteriorate, family supporters and friends bring patients for examination. Patients may have already suffered extensive brain damage by the time they seek therapy. As a result, no therapies will be effective at that time (Mosconi, 2013).

Changes of histology, structure, and function of the brain, which are frequent signs and symptoms of Alzheimer's disease. 20–30 years before the start of AD pathogenesis and neuronal process degradation. Neurodegeneration is a wide word that refers to the advanced damage to structure and function of neurons, as well as the death of neurons. AD is brain disorder caused due to degradation of neural processes (Mosconi, 2013).Changes in brain function and structure are thought to develop 20–30 years before symptoms of Alzheimer's show (Mosconi, 2013). The universal occurrence of dementia is 24 million people, and it is expected to increase after 20 years until 2040, resulting in an expensive disease burden (Reitz et al., 2011). The primary uncontrollable features of this fatal illness are extracellular Amyloid-beta (A) plaque deposits and intracellular neurofibrillary tumor’s (NFTs) (Tang et al., 2019).

The primary structural alterations in AD are plaques which are senile and tangles of neurofibrillary. Amyloid fibrils constitute amyloid-beta (A) peptide. Neurofibrillary masses are made up of hyper-phosphorylated tau protein. There is significant evidence of brain atrophy in the hippocampus. In 1991, three separate research groups proposed that A buildup is the key event in this disease. Amyloid precursor protein (APP), presenilin 1, and presenilin 2 are mutated

genes that encode the main proteins in Amyloid metabolism in hereditary, autosomal, and dominant familial AD (Huang et al., 2020). The factors which contributes to AD are genetics, environment linked possibilities such as diabetes mellitus, oxidative stress, high blood pressure, pollution in the air, excess cholesterol in the bloodstream, abnormal heart rhythm, drugs, smoking, high lipid levels and obesity in middle age, lack of vigorous physical activity, altered glucose metabolism, anxiety, and a low level of education. These risk variables had a significant influence in development of prevention strategies. Unsystematic clinical studies in adults are needed to see if interventions addressing these variables of risk lower likelihood of thinking failure. (Kivipelto et al., 2018).

Primary potential factor in Alzheimer's disease is dysfunctional glucose metabolism and insulin resistance caused by Type 2 diabetes mellitus. Reduced glucose absorption in the brain is the first and most accurate indicator of neuronal shrinkage and dysfunction in Alzheimer's disease. When compared to overall body mass, the brain comprises only 2% of mass of total body. The brain is body's intensive organ of energy. The glucose transporters found in the endothelium of the brain, astrocytes, and neurons are substrates for neural processes. Evidence suggests that impaired brain glucose metabolism is an unchangeable clinical characteristic of this disease. The disease development and the manifestation of clinical symptoms before the loss of intellectual capabilities and alterations in microscopic inspection of tissues contributes to these phenomena. The glucose metabolism in the cerebral cortex and hippocampus of family AD patients was found to be substantially reduced using positron emission tomography (Duran-Aniotz and Hetz, 2016)

Alterations in glucose uptake are the major cause of illness development. Glucose transport through the blood-brain barrier is aided by a few carriers. GLUT-1 is involved in the change in glucose absorption. GLUT-1 is expressed in glia and endothelial cells. GLUT-3 is found in neurons. In animal models of AD, lowering the amount of GLUT-1 in endothelial cells accelerates disease, increasing neuronal degeneration, a deposition, and cerebral degeneration, as revealed by experimental data. The neurodegenerative phase of disease is considered as increase in neuronal dysfunction or aberrant protein aggregation accumulation. The first symptom of Alzheimer's disease is a drop in brain glucose levels. Low glucose absorption or a drop in glucose levels in the brain is a precursor to neuronal degeneration in Alzheimer's disease (Duran-

Aniotz and Hetz, 2016). Glucose level restoration methods, on the other hand, may avoid the start of this disease (Duran-Aniotz and Hetz, 2016).

RESEARCH OBJECTIVES:

AD has risen from obscurity to become one of the most frequent diseases, particularly among the elderly. The frightening rise in AD prevalence is a worrying trend.

The main goal of this research was to discover a link between Alzheimer's disease and glucose metabolism, as well as to evaluate therapeutic potential of targeting impaired glucose metabolism and oxidative stress. These goals will help in the finding and development of new strategies for reducing and preventing Alzheimer's disease.

The major objectives are:

- To understand and uncover linkage between Alzheimer and Glucose Metabolism
- Identification and characterization of proteins involved in glucose metabolism linked AD

CHAPTER 2: LITERATURE REVIEW

2.1 Alzheimer’s Disease (AD)

It is a kind of neurological illness that disturbs the brain. Damage to memory and other cognitive capacities happens in this disease to point,such that it interferes with living on daily basis.60–80% of cases of dementia are of AD. Alzheimer's disease is considered as clumping of beta_amyloid (Aβ)in the brain or tangles of protein tau present in nerve tissue.In brain decrease in acetylcholine (ACh) levels is a major characteristic linked with the development of AD. (Anand et al., 2017). Emerging data shows that hyperphosphorylated tau protein deposition is associated to focused glucose metabolism. When tau is hyperphosphorylated, it separates from microtubules and collects in the, resulting in neurofibrillary tangles (NFTs), Hyperphosphorylation of tau, which results in neurofibrillary tangles, is one of the hallmarks of AD pathogenesis. It mostly accumulated in the neuron's somatodendritic compartment (Adams et al., 2019).

The dementia cause in people with cerebrovascular illness is Alzheimer's disease-related neurodegeneration (AD). It is the second prevalent reason of dementia. Many cases of dementia are caused by mixed aetiologies (which include both neurodegenerative and vascular features), with great occurrence in people over the age of 80, implying that dementia which is mixed is the most common form in elderly populations, as evidenced by mounting neuropathological studies. Some variables can have a varied impact on a person's risk of dementia and Alzheimer's disease reliant on when they are exposed during their lives. When a person is exposed during middle age

to factors that contribute to Alzheimer's, such as hypertension, obesity, and dyslipidaemia, the chance of dementia rises. Other variables, such as nutrition, cardiovascular risk factors, and age, have a long-term effect on risk (Kivipelto et al., 2018)

Figure 2.1*: Factors and events associated with Alzheimer's disease : This shows the events and changes which occur during AD such as amyloid precursor protein and neurofibrillary tangles.*

2.2 Subtypes Classification of Alzheimer's Disease

This disease is classified into subtypes based on two key factors: age of onset and genetic background. Genetic or familial Alzheimer's accounts for 1% of Alzheimer. (eFAD). Autosomal dominant changes in the three genes PSEN1, PSEN2, and APP cause this disease. Sporadic Alzheimer's type defined as having no known genetic alterations.

There are two categories based on their onset age familial and sporadic instances The late-onset kind contains sporadic occurrences of Alzheimer's disease, whereas the early-onset form includes familial cases. Although limits for the age of onset are random, with age the chance of getting AD rises.

Figure2.2: *Types of Alzheimer disease(AD)*

Figure 2.3 *: Epidemiology of Alzheimer's disease subtypes.*

Late-onset Alzheimer's disease constitutes the largest percentage of the patients suffering from AD which is 95% of the total AD cases. are Early-onset Alzheimer's disease constitutes about 4% of the AD cases,and early-onset familial AD constitutes 1% of all the AD cases . (Shafiq 2019).

AD is both complicated and diverse. In this disease, a number of genes must be discovered and verified. Furthermore, while there is a 70% hereditary risk of getting Alzheimer's disease, familial AD constitutes less than 1% of the disease. The two basic types of AD are (1) early onset Familial AD which onset early (2) late AD, often known as form which is sporadic, although the important is many features of this distinction remain unclear. Three genes, however, have proven crucial in our knowledge of the process of this disease. Mutations in the APP, presenilin-1 gene (PS1), and presenilin-2 gene (PS2), in particular, produce a dominant autosomal type of Alzheimer's disease with a new start. These changes result in rise in Ab production or in Ab42 (Davinelli et al., 2011).

2.2.1 Familial AD

Familial are 1–5% of all AD cases , and it possess fast start caused by genes alterations that cause accelerated amyloidogenic processing and tau hyper-phosphorylation (Pilipenko et al., 2020).

2.2.2 Sporadic AD

In early stages of dementia extreme changes initially can be detected. The modifying approaches of disease creates more therapeutic chances before start of severe impairment in cognition. The sporadic form of AD accounts for 95–99 percent of Alzheimer. In the early- stages of dementia early pathological changes can be identified. Decrease in tolerance of glucose and decreased

brain metabolism of glucose were identified before initial stage of spAD, indicating a two-way connection among diabetic and Alzheimer patients. (Pilipenko et al., 2020).

2.3 Rapidly progressive AD

It is a neurological illness that progresses slowly over 8 years with slowly increasing symptoms rigorousness making it easy to distinguish from dementia that progresses quickly. The cognitive deterioration was measured using the Mini Mental State of Examination, which revealed loss fewer tof 6 MMSE units annually on average. The quickly progressing dementia mimic atypical Alzheimer's disease. The average cognitive deterioration in these patients is greater than 6 MMSE units each year. In these patients, the post-diagnostic survival period is about 4 years, compared to 8 years in normal spAD cases. Cases of Alzheimer's disease are initially misdiagnosed as Creutzfeldt-Jakob disease, but post-mortem pathological investigations eventually reveal the Alzheimer's pathology.

There is currently a lack of research on rpAD. In 1989, rapidly progressive AD (rpAD) copying Creutzfeldt–Jakob disease was reported first time.In 2004 next case was repoted with the discovery of 14-3-3 in CSF and following classification of the patient as a CJD case, where postmortem pathological examination indicates the presence of AD. (Reinwald, Westner, & Niedermaier, 2004). Jayaratnam and colleagues found 14-3-3 positive in another case of fast progressing AD.(Jayaratnam, Khoo, & Basic, 2008).(Shafiq 2019).

2.4 Outcome of Alzheimer’s Disease (AD)

Proteins usually soluble assemble form oligomers, fibrils, and other structures in Alzheimer's disease, as evidenced by data of genes, biochemical, clinical, and biomarkers. This mechanism is connected to harmfulness and neuronal loss. The extracellular accumulation of the amyloid beta in brain is the fundamental initial incident in AD. There is considerable evidence that AD pathology, including the beginning and gradual accumulation of insoluble forms of A and tau, begins 10-15 years before to the onset of cognitive loss associated with AD. The initial clinical signs of AD are evident, a build-up has reached its peak, and generally significant degree of tangles of neurofibrillary. The considerable neuronal and loss in synapses in numerous areas of brain that are important for memory and other cognitive processes. Preclinical AD refers to the

time when Alzheimer's disease pathology is collecting but discernible cognitive impairment is absent.(Vlassenko and Raichle, 2015).

It is a polygenic and complicated illness; the biology of the disease is not well understood. The following are the neuropathological hallmarks of AD:

Figure 2.4*: Outcome of Alzheimer's Disease(amyloid beta plague accumulation,acetylcholine concentration decrease results in cognitive impairment.*

The cause of AD is deposition of β-amyloid (Aβ) in the brain, as well as other brain abnormalities such as neurofibrillary tangles, dystrophic neurites, synaptic loss, and so on. Neurotoxicity is caused by intracellular fibrillary oligomeric forms of Aβ peptide produced earlier in the disease's course, rather than external amyloid plaques. The basic premise that the illness is caused by an Aβ accumulation, oligomerization, and toxicity is, however, unaffected. Despite the fact that there must be a fundamental cause or trigger, such as hereditary factors or undiscovered environmental toxins, neurodegeneration in Alzheimer's disease starts at level of amyloid beta oligomers or fibrils (Grieb, 2016)The factors connected with Alzheimer's disease are of two types. Non-genetic risk factors (factors with no proven gene connections to Alzheimer's disease) and genetic risk factors (genes that have been linked to various elements of Alzheimer's disease). Cerebrovascular diseases, hypertension (related degeneration of the blood-brain barrier), type 2 diabetes, lipid levels in plasma, health, and traumatic head injury are all non-genetic risk factors. Several genetic risk factors, namely Amyloid precursor protein, Tau, and metabolism of cholesterol, immunological response, endocytosis, and cytoskeleton of axon , have been linked to various features of this disease.The researched risk factors is the APOE polymorphism (Reitz and Mayeux, 2014).

Figure 2.5 : *Factors associated with Alzheimer's Disease*

Tangles of neurofibrillary (NFTs, made up of aberrant tau) plaques of amyloid [made up of extracellular collections of amyloid-β (Aβ) are extreme markers of Alzheimer's disease. The NFT protein tau is linked to microtubules for stability. Alzheimer's disease patients' cognitive deficits were linked to tau pathology and synaptic loss. The amyloid plaque component A is formed when the membrane protein APP (Amyloid precursor protein) is cleaved by the -secretase BACE1 (-site amyloid precursor protein cleaving enzyme 1) and the -secretase complex. Dysregulation, abnormal modification, and accumulation of these protein complexes in the brain are key illnesses that cause Alzheimer's disease.

Most types of AD are other than genetic and onset late from a genetic viewpoint, although familial forms of AD starts early and it exist and are often caused by changes in APP. The molecular processes that cause sporadic types of Alzheimer's disease are yet unknown. To mention a few processes, inflammation, regulation of hormones, malfunction of mitocondria, and lysosomal not functioning properly have all been involved. Microglial participation is also becoming more genetically evident. Aging, risk factors involving genes such as APOE-4 carrier of allele, disturbing injury of brain, cardiovascular risk factors, and many environmental risk are the primary causes for developing of this disease (Rotermund et al., 2018).

2.5 Molecular Basis of Glucose Metabolism

Glycolysis process, Krebs cycle, and oxidative phosphorylation in the mitochondria turns glucose into ATP. Glucose transporters transfer glucose from the bloodstream to the tissues under aerobic circumstances. It is subsequently phosphorylated into) by the The enzymes hexokinase and glucokinase,converts glucose-6-phosphate (G-6- P) into pyruvate and then further processed through the glycolytic pathway. Pyruvate enters mitochondria, where it is degraded by enzymes during oxidative phosphorylation (OXPHOS) (Mosconi 2013).

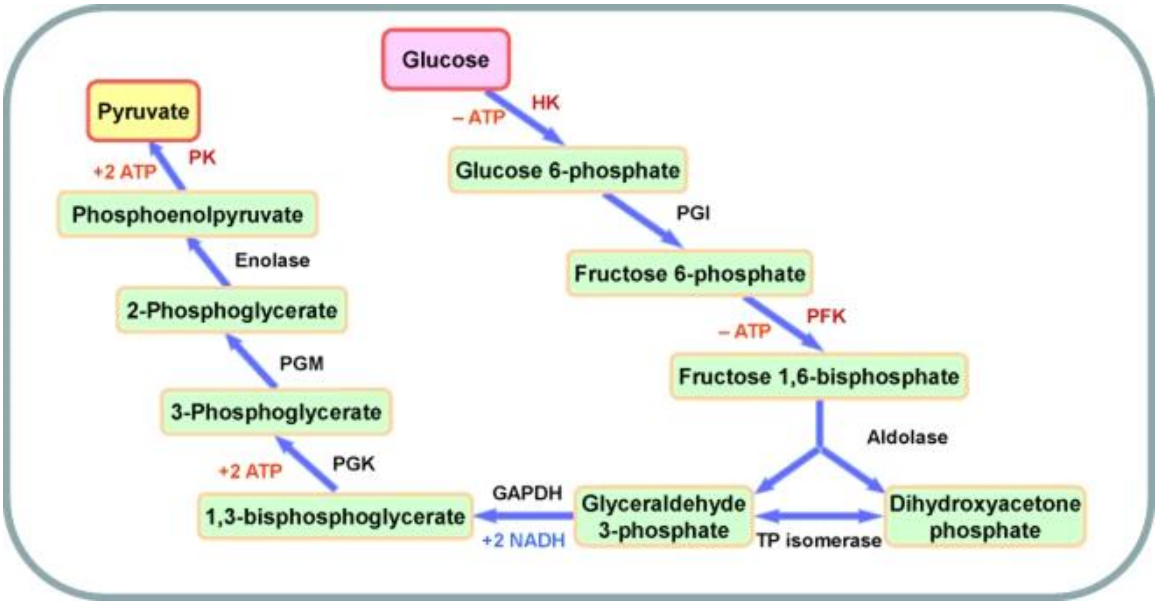

Figure 2.6 : *Schematic diagram of Glycolysis.(Li, Gu et al. 2015)*

Above diagram illustrates the ten stages and ten particular enzymes, which are hexokinase (HK), phosphoglucose isomerase (PGI), phosphofructokinase (PFK), aldolase, triosephosphate isomerase (TPI), glyceraldehyde 3 phosphate dehydrogenase (GAPDH), phosphoglycerate kinase (PGK), phosphoglycerate kinase(PK).

Glucose is the most essential energy generating chemical in life. Glycolysis in anaerobic settings, full oxidation in aerobic situations, and the pentose phosphate pathway make up glucose metabolism. Glycolysis is the metabolic route in which glucose is converted to pyruvate in the cytoplasm, which is then converted to adenosine triphosphate (ATP). By the 1940s, the entire glycolysis route, which consists of ten chemical processes mediated by different enzymes, had been described (Li et al., 2015).The process of oxidative phosphorylation produces a lot of ATP. It is required for cellular homeostasis to operate properly. When pyruvate reacts with oxygen creates group of acetyl, carbon dioxide is released. The group of acetyl (CH3CO) joins coenzyme A results in formation of acetyl coenzyme A, which subsequently go in the Krebs cycle. The acetyl group is oxidised and create two molecules of carbon dioxide throughout this series of events, and to four electron carrier molecules energy is released, which eventually results in the electron transport chain. (Mosconi 2013).

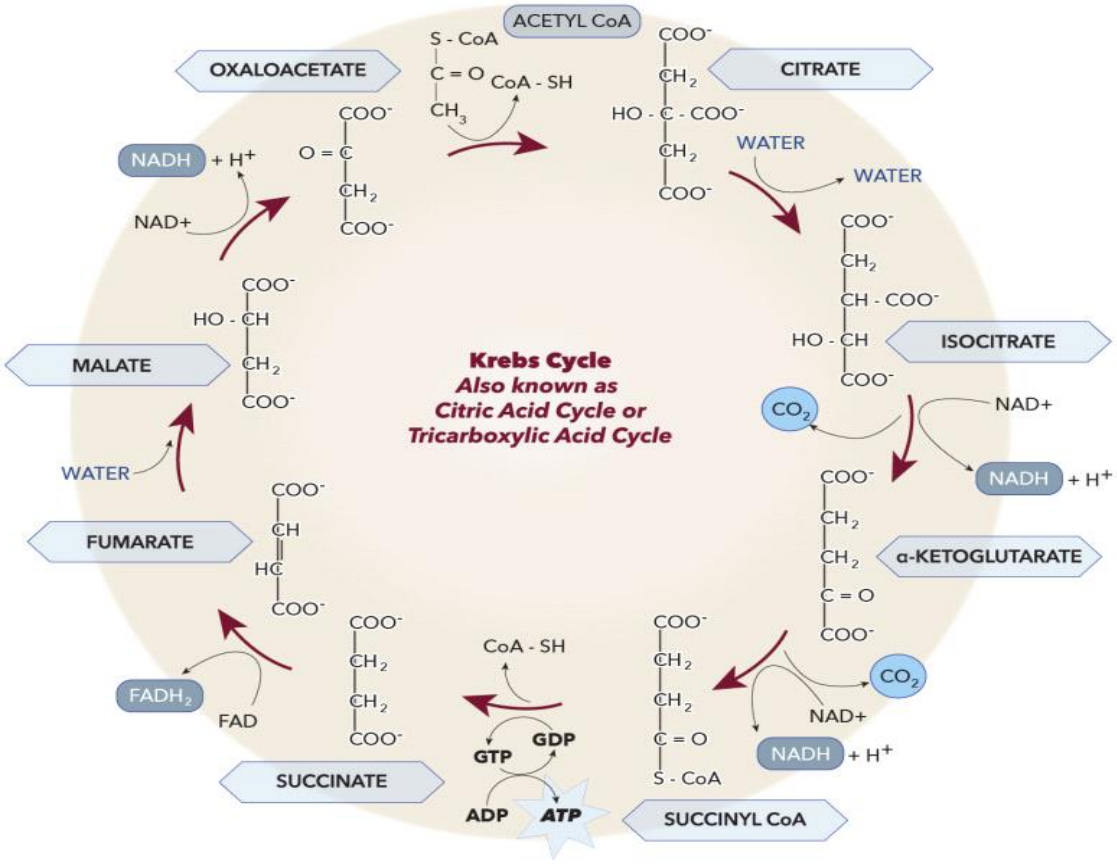

Figure 2.7 : *Schematic diagram of Kreb Cycle.(Abolhassani, Leon et al. 2017).*

The ETC is made up of four membrane-bound complexes buried in inner mitochondrial membrane and electrically linked by electron carriers. NADH dehydrogenase (Complex I), succinate dehydrogenase (Complex II), cytochrome bc1 complex (Complex III), and cytochrome c oxidase (Complex IV) are the four complexes (COX, Complex IV). Complexes I, III, and IV are proton pumps that transport H+ across the IMM against the concentration gradient, generating a proton gradient from the matrix to the intermembrane space, while moving electrons down the ETC. This proton gradient is used by FoF1-ATP-synthase (Complex V of the ETC) to generate ATP via OXPHOS of ADP to ATP. The energy-demanding process in the cell is ATP hydrolysis (Mosconi 2013).

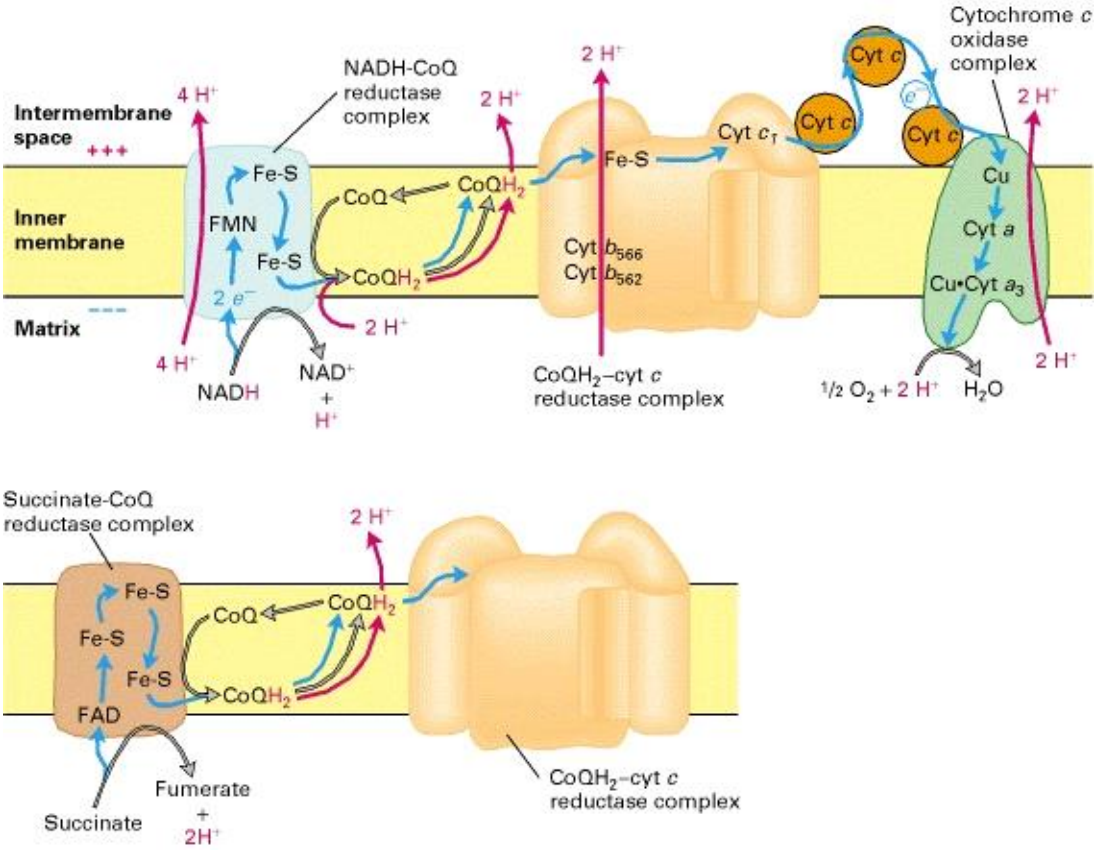

Figure 2.8 : *Pathway of Oxidative Phosphorylation via Electron transport chain (Lodish, Berk et al. 2000)*

Each of the chain's four major multiprotein complexes is found in the inner mitochondrial membrane and contains a number of different electron carriers. Electrons are transported between the complexes via coenzyme Q (CoQ) and cytochrome c. The energy generated as electrons travel through three of the complexes is enough to propel H+ ions across the membrane, producing a proton-motive force (Deshpande and Mohiuddin, 2019).

2.6 Altered Glucose Metabolism

As evaluated in vivo with positron emission tomography, Alzheimer's disease (AD) is characterised by reduced cerebral glucose metabolism, notably in the temporoparietal areas (PET) (Adams et al., 2019). The variables that impact the start of AD pathology, such as Aβ aggregation, must be studied in order to understand the pathological initiation of the AD process. Metabolic dysfunction, which appears to be linked to the reduction in total glucose consumption, is a key characteristic of the developing brain disease. Reduced glucose consumption (up to

50%) in human patients at an early stage is a well-known pathological characteristic of Alzheimer's disease. During the early stages of Alzheimer's disease, decreases in global brain or parieto-temporal glucose utilisation (45-50%) are higher than declines in blood flow and oxygen consumption (20-30%). Only in the latter stages of Alzheimer's disease can variations in blood flow and oxygen use resemble changes in glucose utilisation. One of the primary causes of Alzheimer's disease is an early mismatch between glucose intake and blood flow/oxygen consumption (Vlassenko and Raichle, 2015).

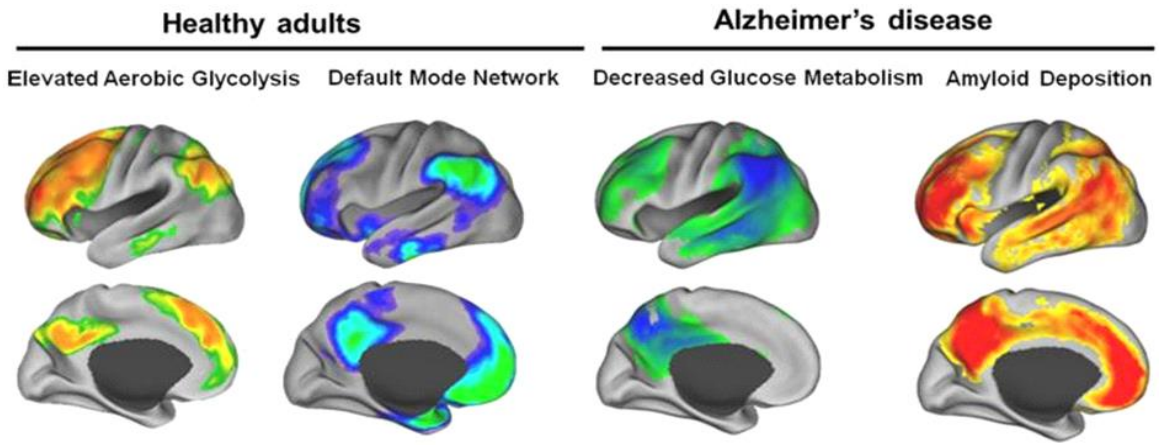

FIGURE 2.9 : *Decreased Glucose metabolism in Alzheimer (Vlassenko and Raichle 2015)*

Images (left to right) contrasting the cortical distribution of increased AG and task-induced activity reductions in the DMN in healthy people with regions of impaired glucose metabolism and Aβ plaque accumulation in Alzheimer's disease patients (Vlassenko and Raichle, 2015).Glucose transporters take up glucose, which is an important energy source for brain function. An unchanging pathogenic characteristic of Alzheimer's disease is impaired brain glucose metabolism (AD). This phenomenon is thought to play a role in disease development and the emergence of clinical symptoms decades before cognitive impairment and histological changes appear (Duran-Aniotz and Hetz, 2016).

Sporadic Alzheimer's disease (spAD) is a metabolic illness characterised by poor glucose consumption by the brain, as shown by neurodegenerative research over the last two decades. As a result, Grieb proposed the glucose cascade theory as the cause of sAD. Reduced glucose transport causes deficiencies in the synthesis of functional glucose transporters (GLUTs): GLUT-1, which participates in glucose transport into the brain and uptake into glial cells, and

GLUT-3, which is responsible for glucose absorption into neurons. Glucose hypometabolism causes insulin resistance and cellular death. Overactivation of glycogen synthase kinase-3 (GSK-3) has been related to glucose intolerance and memory impairment in model animals, and is thought to be the connection between alterations in glucose turnover and early pathogenic events such neuroinflammation (Pilipenko et al., 2020).

These occurrences occur during the prodromal phases of spAD, when moderate cognitive impairment (MCI) may be present. The neuroinflammation events astrogliosis and microgliosis aggravate the neurodegenerative process triggered by glucose hypometabolism. Synaptic plasticity is disrupted, neuronal death occurs, and cell-cell communication is disrupted, resulting in cognitive impairment and increased acetylcholine cleavage. A combination of poor spatial learning/memory and social behaviour is a distinct characteristic of Alzheimer's disease. Reduced glucose tolerance and decreased brain glucose metabolism were identified at the prodromal stage of sAD, indicating a bi-directional connection between AD and diabetes (Pilipenko et al., 2020)

Figure 2.10: *Schematic Diagram of link between Alzheimer and Glucose Metabolism*

It is the most common kind of dementia in persons over 65, and type 2 diabetes mellitus is a metabolic disorder that affects 382 million adults globally. The brain's primary source of energy is glucose, which accounts for 25% of the body's glucose. Positron Emission Tomography (PET) scanning is a popular technique used for diagnosis and follow-up in AD and glucose metabolism. Epidemiological and pathophysiological investigations have shown a connection between AD and diabetes, particularly in relation to insulin resistance (Calsolaro and Edison, 2016).Changes in oxidative metabolism in Alzheimer's disease were discovered in 1965. Several investigations have shown the presence of severe oxidative stress in brain tissue, fibroblasts, and blood platelets in Alzheimer's disease. At post mortem, all cellular macromolecules (protein, DNA, lipids) are detected in an oxidised state, indicating severe oxidative stress in AD brains. In the deterioration process of Alzheimer's disease, oxidative stress is most apparent in the brain areas, particularly in the form of decreased COX activity in the parieto-temporal, frontal, and posterior cingulate cortices, as well as the hippocampus (Mosconi 2013).

Abnormalities in brain metabolic activity are the first and most well-documented changes in dementia. In vivo investigations of glucose intake utilising positron emission tomography have shown that cerebral energy metabolism is impaired, according to the majority of evidences. Alzheimer's disease has been linked to a persistent pattern of decreased temporoparietal glucose metabolism. However, these investigations do not distinguish whether lower deoxyglucose absorption under these conditions reflects a restricted metabolic capability of the brain or a simple reduction in energy demand by the sick organ. They also don't say if the decreased glucose absorption is related to neuronal death or a functional impairment in the brain (Bigl et al., 1999).

Reduced GLUT1 and GLUT3 glucose transporter concentrations, reduced brain metabolic rate for glucose, impaired synthesis of acetylcholine and other neurotransmitters, and decreased activity of certain glucose breakdown enzymes have all been observed. However, conflicting results have been published for a number of enzymes. Hexokinase (HK) activity has been found to be reduced in the brain, fibroblasts, leukocytes, and microvessels of Alzheimer's patients. In numerous investigations, the activity of 6-phosphofructo-1-kinase (PFK) was reported to be significantly reduced in postmortem AD brains (Bigl et al., 1999)

A re-evaluation of PFK activity in the frontal and temporal cortex of AD patients matched to controls revealed a substantial rise in this enzyme's specific activity utilising an improved tissue extraction and testing method. This finding was unexpected, given both the neurodegeneration and the decreased cerebral glucose intake seen in this disease. Plastic changes, are visible in brains of AD.Increased numbers of reactive astrocytes are an unchanging characteristic of AD pathogenesis (astrocytosis). Astrocytes may play a role in neurotrophic support. Immunohistochemistry of glial fibrillary acidic protein reveals abundant glia fibrils produced by reactive astrocytes. Changes in the activity of major glycolytic enzymes have been identified as causes of AD in recent research (Bigl et al., 1999).

The hypothesis of amyloid cascade has controlled Alzheimer's study for a long time. Aß is regulated by mitochondria and cell bioenergetics, and any alterations in mitochondrial function and cell bioenergetics in sporadic AD occur prior to Aß modifications. From a molecular standpoint, disrupted mitochondrial activity may increase APP processing to amyloidogenic derivatives or Aß synthesis by increasing free radical generation. During the course of LOAD, a

poor energy metabolism, increased oxidative damage due to faulty mitochondrial activity, and a change in the overall oxidative milieu may modify the overall oxidative microenvironment, predisposing neurons to degeneration and dysfunction (Mosconi 2013).The link between ageing and Alzheimer's disease, which is strongly linked to many features of mitochondrial function, has been used to imply that mitochondria may be at the top of LOAD . The model's main assumptions are that a person's genes define the standard of mitochondrial function, that durability dictates how mitochondria change with age, and that significant alterations in function of mitocondria begin additional pathologies associated with Alzheimer's disease (Mosconi 2013). Investigations of brain glucose metabolism, particularly using neuroimaging methods in conjunction with proteomic, genomic, and mitochondrial biochemistry, are well suited to investigate this theory. The significance of oxidative stress and abnormal glucose metabolism in this disease is becoming more well acknowledged (Mosconi 2013).

CHAPTER 3: MATERIALS AND METHODS

MATERIALS

% Acrylamide	12.5%	4% Stacking Gel
30% Acrylamide (ml)	12.5	1.3
1 % Bisacrylamide(ml)	3.1	1.5
1.5 M Tris, pH 8.7(ml)	8.1	-
0.5 M Tris pH 6.7 (ml)	-	1.25
20% SDS (ml)	0.2	65 (µl)
H20 (ml)	6.2	5.725
TEMED (µl)	10	10
10% Ammonium persulfate (µl)	225	150

METHODOGY

1.Sample Preparation/Collection

2.Ethic Statement

3.Protein Extraction and trypsin digestion

4.Mass Spectrometry

5.Immunoblot analysis

6.Statistical Analysis

METHODS

3.1 SAMPLE PREPARATION / COLLECTION

The Surveillance Units of Germany and Spain regarding Prion disease donated the brain samples, which included SPAD and non-demented control cohorts. The samples of brain tissue were processed. The frontal cortex of SPAD patients (4M/5F) with a mean age of 77.3 years was extracted. Goettingen patient data was collected.

The samples from frontal cortex region cohorts with sporadic AD and dementia with frontotemporal lobar degeneration were given by the Brain Bank of the Institute of Neuropathology (HUB-ICO-IDIBELL Biobank) and the Biobank of Hospital Clinic-IDIBAPS Spain. Frontal cortex samples from individuals with sporadic subtypes were supplied by the Department of Neurology at the University Medical Centre in Gottingen, Germany. The SPAD cohort consisted of patients who rigorously met the following inculding criteria:

1. Early diagnosis of prion disease established on clinical criteria.

2. In the absence of data on CERAD / Braak staging, the examining neuropathologist's assessment and diagnosis were recognised as an acceptable neuropathological diagnosis.AD

pathological characteristics, such as higher Braak and CERAD stages justifying AD diagnosis, neuropathological diagnosis of Alzheimer's disease is made.

3. Elimination of prion disease and important, possible reasons of fast dementia (widespread cortical Lewy body, tumors, severe vascular illness, stroke, inflammation, etc.) based on neuropathological evaluation.

4. There should be no family history of Alzheimer's disease (autosomal dominant mutations). If all of the above-mentioned inclusion criteria were met, patients of all ages were included in the research. One-centimeter thick portions of one of the hemispheres were removed. Dissected tissues were quickly frozen for biochemical studies and then stored at -80C for subsequent use. Immersion in 4 percent buffered formalin for three weeks fixed the opposite hemisphere. Later, morphological and neuropathological characterizations were performed, and so on.

spAD					
No.	**Case**	**Clinical Diagnosis**	**Age**	**Gender**	**Disease duration(y)**
1	spAD1	AD	78	Male	>4
2	spAD2	AD	72	Female	>4
3	spAD3	AD	82	Female	>4
4	spAD4	AD	56	Female	>4
5	spAD5	AD	87	Male	>4
6	spAD6	AD	85	Female	>4
7	spAD7	AD	93	Male	>4
8	spAD8	AD	74	Female	_
9	spAD9	AD	82	Male	_
Cont					
No.	**Case**	**Clinical Diagnosis**	**Age**	**Gender**	**Disease duration(y)**
1	Cont1	N	69	Male	_
2	Cont2	N	68	Male	_
3	Cont3	N	64	Male	_
4	Cont4	N	67	Male	_
5	Cont5	N	74	Male	_
6	Cont6	N	86	Male	_
7	Cont7	N	73	Female	_
8	Cont8	N	61	Male	_
9	Cont9	N	77	Male	_

3.2 ETHIC STATEMENT

Samples were controlled in accordance with local regulations (Ley de la Investigación Biomédica de 2013 and Real DecretoBiobancos de 2014). After local ethical boards at the University Medical Centre in Gottingen gave their clearance, the sporadic (AD) cohort was collected. After receiving permission from the Internal Review Board SMME, NUST, the process was followed.

3.3 PROTEIN EXTRACTION AND TRYPTIC DIGESTION

Tissue slices were homogenized in ice-cold lysis buffer I using a steel beads tissue disruptor to a 10% w/v for immunoblotting or entire proteome mass spectrometric analysis, then supplemented with protease inhbitor. Overnight homogenates were raised at 4°C. At 40,000 xg at 4C for 30 minutes after ultracentrifugation, the supernatants were collected and utilized for downstream applications (Beckman Coulter ultracentrifuge).

The Bi-phasic gels having a 4% stacking gel and a 12% resolving gel had been used to separate proteins on the basis of their molecular weight. Separates comprising similar protein quantities had been cooked to 95°C for 5 minutes in a thermomixer with the appropriate volume of 4x Laemmli buffer. Samples were placed on top of the gels together with an appropriate molecular weight protein marker (Bio-Rad dual colour precision plus protein standards). The loading dye remained electrophoresed at 100 V till it reached 1 cm of the resolving gel. Running buffer (1x) made by diluting 10x running buffer stock and proteins were excised from gel and excised band was digested with trypsin enzyme.Gels were stained with Comassie blue overnight. The bands of interest was excised from commassie stained gels, in-gel protein digested, and recovered peptides were submitted to mass spectrometric based MS/MS protein identification analysis. The two sequenced peptides per protein spot were required for acceptance.

3.4 MASS SPECTROMETRY

Either frontal cortex homogenates (50 µg protein per sample), density variant fractions (30 µL) or Co-IP eluates from density variant fractions (30 µL each) were loaded onto 4-12% NuPAGE Novex Bis-Tris Mini gels (Invitrogen) and run into the gel for 1 cm. Following Coomassie staining, the protein-stained gel areas were excised, diced, and washed in ddH2O. After having been washed, the gel slices were reduced with reduciing buffer (10 mM DTT in 100 mM NH4HCO3) by being incubated for 30 min at 56°C, followed by alkylation with alkylation buffer (55 mM IAA in 100 mM NH4HCO3) at RT in the dark for 60 min. Gel slices were then incubated in acetonitrile (ACN) for 15 min and dried in a SpeedVac to remove excess solvent. Dried gel slices were stored at -20°C before further use. For mass spectrometric identification of Co-IP from whole brain homogenates, the eluates were loaded on to 12% SDS polyacrylamide gels and gel electrophoresis continued until the loading dye had reached the bottom. Gels were then silver-stained, and the silver-stained bands were excised and processed for the peptide extraction with the protocol detailed above.

3.5 STATISTICAL ANALYSIS

Graphpad prism 6.0 was used for simple statistical analysis.Densitometric study of western blots and 1-DE gels was performed by means of graphpad prism.

3.6 BIOINFORMATIC ANALYSIS

The efficient enrischment of detected proteins from MS/MS analysis Uniprot/SwissProt database was used.Based on Uniprot SwissProt data base annotations from high density fraction datasets and global proteome datasets were automatically grouped representing singular physiological category for proteomics.Homosapiens database was used as reference database.

CHAPTER 4: RESULTS

4.1 Identification of Unique Peptide Sequences Through Scaffold

For protein identification, one sample from the AD group and one sample from the control group were analysed by using MS. The generated data files were converted to the SF3 file format and exported to the Scaffold database search tool (version). The below figure displays the exported raw MS/MS data of ALDOA protein obtained from the Scaffold database. It shows the identified peptides of the ALDOA protein. (a) shows that ALDOA protein was obtained from homo sapiens with a molecular weight of 39,420.6D. There were 14 exclusive unique peptides, from which 16 exclusive unique spectra were identified with an amino acid of 179 out of 364 and having 49% coverage. Amino acids that matched MS/MS spectra are in yellow. (b) It shows the probability and sequence coverage of ALDOA protein.

a

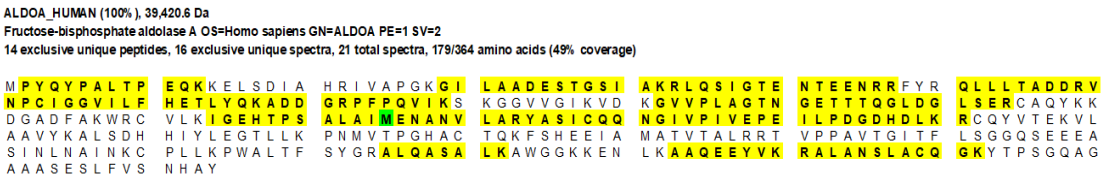

b

Sequence Coverage	Protein	Accession	Category	MS/MS Sample	Bio Sample	Prob	%Spec	#Pep	#Uni...	#Spec	%Cov	m.w.
	Fructose-bis...	ALDOA_HUMAN	10	A_Noor_211217_020318_10.msm (F082604)	A_Noor_211217_Human_10	100%	0.11%	14	16	21	49%	39 kDa
	Fructose-bis...	ALDOA_HUMAN	09	A_Noor_211217_020318_09.msm (F082603)	A_Noor_211217_Human_09	100%	0.010%	2	2	2	6.0%	39 kDa
	Fructose-bis...	ALDOA_HUMAN	08	A_Noor_211217_020318_08.msm (F082602)	A_Noor_211217_Human_08	100%	0.0053%	1	1	1	3.8%	39 kDa
	Fructose-bis...	ALDOA_HUMAN	06	A_Noor_211217_020318_06.msm (F082600)	A_Noor_211217_Human_06	98%	0.0051%	1	1	1	3.8%	39 kDa
	Fructose-bis...	ALDOA_HUMAN	04	A_Noor_211217_020318_04.msm (F082598)	A_Noor_211217_Human_04	100%	0.022%	4	4	4	9.9%	39 kDa
	Fructose-bis...	ALDOA_HUMAN	03	A_Noor_211217_020318_03.msm (F082597)	A_Noor_211217_Human_03	100%	0.038%	7	7	7	27%	39 kDa
	Fructose-bis...	ALDOA_HUMAN	02	A_Noor_211217_020318_02-2.msm (F082596)	A_Noor_211217_Human_02...	100%	0.011%	2	2	2	13%	39 kDa
	Fructose-bis...	ALDOA_HUMAN	05	A_Noor_211217_020318_05.msm (F082599)	A_Noor_211217_Human_05	93%	0.00%	0	0	0	0.00%	39 kDa
	Fructose-bis...	ALDOA_HUMAN	01	A_Noor_211217_020318_01.msm (F082594)	A_Noor_211217_Human_01	89%	0.00%	0	0	0	0.00%	39 kDa

Figure 4.1: *(a) This figure shows the identified peptides of the ALDOA protein.0.1(b) It shows the probability and sequence coverage of ALDOA protein.*

Mass Spectrometry

MS identified the mass to charge ratio of molecules present in the sample of AD patients. The study demonstrated the quantitative profiling was done to investigate the interaction of ALDOA protein. A graphical representation of sample spectrum produced by Mass Spectrometry. The peptide data were searched against the UniprotKB homo sapiens reference proteome using the MS/MS ion search engine. In the above graph, b- ions are numbered from left to right on the N-terminus and y-ions are numbered from right to left on the C- terminus.

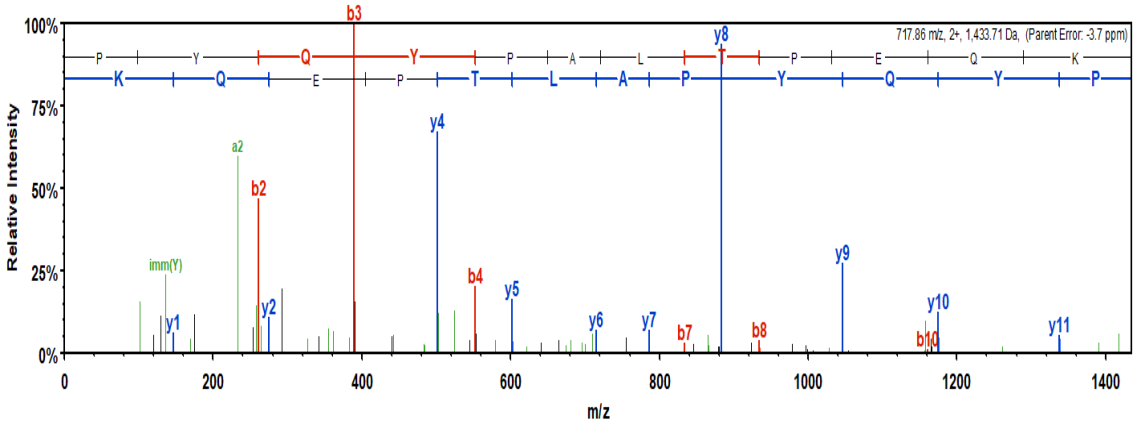

Figure 4.2: *This is a simplified mass spectrum of ALDOA protein which shows the mass to charge ratio on the x-axis and relative intensity on the y-axis.*

The potential ions which match the spectrum are coloured. Red boxes show the b ions while Blue ions show the Y ions and Green boxes refer to the neutral loss or similar fragmentation patterns.

B	B Ions	B+2H	B-NH3	B-H2O	AA	Y Ions	Y+2H	Y-NH3	Y-H2O	Y
1	98.1				P	1,434.7	717.9	1,417.7	1,416.7	12
2	261.1			243.1	Y	1,337.7	669.3	1,320.6	1,319.7	11
3	389.2		372.2	371.2	Q	1,174.6	587.8	1,157.6	1,156.6	10
4	552.2		535.2	534.2	Y	1,046.6	523.8	1,029.5	1,028.5	9
5	649.3		632.3	631.3	P	883.5	442.2	866.5	865.5	8
6	720.3	360.7	703.3	702.3	A	786.4	393.7	769.4	768.4	7
7	833.4	417.2	816.4	815.4	L	715.4	358.2	698.4	697.4	6
8	934.5	467.7	917.4	916.5	T	602.3		585.3	584.3	5
9	1,031.5	516.3	1,014.5	1,013.5	P	501.3		484.2	483.3	4
10	1,160.6	580.8	1,143.5	1,142.6	E	404.2		387.2	386.2	3
11	1,288.6	644.8	1,271.6	1,270.6	Q	275.2		258.1	257.2	2
12	1,434.7	717.9	1,417.7	1,416.7	K	147.1		130.1		1

Figure 4.3: *Figure illustrates the fragmentation table that displays the same information as the above spectrum in a spreadsheet format.*

The glycolytic enzyme that catalyzes the reversible conversion of fructose-1,6-bisphosphate to glyceraldehyde 3-phosphate and dihydroxyacetone phosphate is fructose-bisphosphate aldolase A.The progression of multiple types of cancers and Alzheimer is caused by disruption of this gene. In metabolic pathway of glycolysis and glucogenesis this protein plays key role.

The degenerative progression of Alzheimer's disease is linked to an energy metabolism. The cognitive impairment induced by diabetes mellitus. It can lead to metabolic irregularities and

glucose transport problems in the body. Diabetic individuals should focus on treatment methods that regulate glycaemic levels or restore glucose metabolism to minimise the occurrence of AD. Preventive strategies are being developed to help postpone and reduce the start and course of Alzheimer's disease. These findings point to proteins implicated in faulty glucose metabolism and Alzheimer's disease. We utilised two software programmes, String and Scaffold, to identify such proteins. The STRING database contains data from a variety of sources, including experimental data, computer prediction approaches, and public text collections. It is open to the public and is updated on a regular basis. The tool also highlights functional enrichments in protein lists submitted by users. GO, Pfam, and KEGG are examples of functional categorization systems. Samples are compared using scaffold software to determine biological significance. Determine which isoforms and protein PTMs are regulated. Investigate the spectrum's finer points and numbers. Identify proteins with confidence and intuition. Make a list of all the proteins you want to target. Sort proteins according to their molecular function or organelle. Utilize batch processing with a high throughput.The present experimental study involves the characterization of glucose linked proteins with progression of Alzheimer using Bioinformatics tools including String and Scaffold. The identified proteins involve Fructose Bisphosphate Aldolase A, Fructose Bisphosphate Aldolase C, Enolase, Glyceraldehyde 3 Phosphate, Pyruate kinase, Malate Dehydrogenase Mitochondrial, Phoshoglycerate kinase 1.

The reversible conversion of fructose-1,6-bisphosphate to glyceraldehyde 3-phosphate and dihydroxyacetone phosphate is catalyzed by fructose-bisphosphate aldolase protein A, a glycolytic enzyme. Disruption of this gene has also been linked to the development of malignancies and Alzheimer's disease. This protein is important in the glycolysis and glycogenesis metabolic pathways.The capacity to execute mechanistically different activities has led to the identification of Glyceraldehyde 3 Phosphate protein as a moonlighting protein. It is a glyceraldehyde-3-phosphate dehydrogenase and a nitrosylase, which means it is involved in glycolysis and nuclear processes. With this protein Alzheimer's disease and Huntington's disease are linked to this disease.

Enolase enzymes are cytosolic carbon-oxygen lyases that play an important role in glucose metabolism. Enolase has recently been shown to have a range of regulatory roles other than glycolysis and gluconeogenesis, connected to hypoxia, ischemia, alzheimer.Pyruvate kinase is

glycolysis enzyme that is engaged in the last stage. The phosphate group transfer from phosphoenolpyruvate (PEP) to adenosine diphosphate (ADP), resulting in one pyruvate and one ATP molecule.

Malate Dehydrogenase involves one molecule of pyruvate and one molecule of ATP and appears in many metabolic pathways, including the kreb cycle.

The moonlighting protein based on its ability to perform mechanistically distinct functions is Glyceraldehyde 3 Phosphate protein .Glyceraldehyde-3-phosphate dehydrogenase play role in glycolysis and nitrosylase activities, playing a role in nuclear functions, respectively. Alzheimer and Huntington disease are disorder associated with this protein..

The exported raw MS/MS data of Glyceraldehyde-3-phosphate dehydrogenase protein obtained from the Scaffold database. It shows that G3P protein was obtained from homo sapiens with a molecular weight of 36,053.4Da. There were 12 exclusive unique peptides, from which 18 exclusive unique spectra ,31 total spectra were identified with an amino acid of 168 out of 335 and with a 50% coverage. Amino acids that matched MS/MS spectra are in yellow.

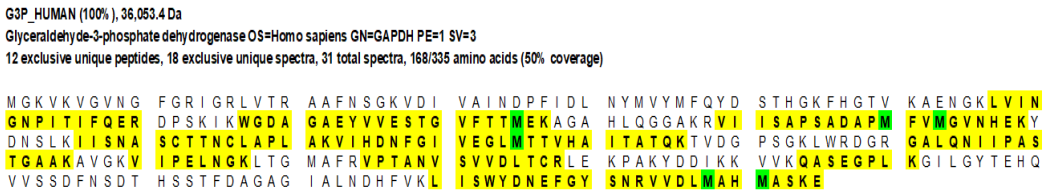

Figure 4.4:*The figure demonstrates the identified peptides of the G3P protein.*

Valid	Weight	Sequence	Prob	Mascot Ion score	Masc...	Masc...	NTT	Modifications	Observed	Actual Mass	Charge	Start	Delta Da	Stop	Delta PPM	# Ot...	Rete...	Other Prot...	Intensity	Spectrum ID	TIC
☑	1.0	(K)LVTMGNPITIFQER(D)	100%	87.1	25.0	78.6	2		807.45	1,612.89	2	67	-0.0011	80	-0.66	0				Elution from: 37.20 to 37.97 period: A_Noor_211217...	6445000
☑	1.0	(K)LVTMGNPITIFQER(D)	100%	49.0	25.0	45.7	2		807.45	1,612.89	2	67	-0.0011	80	-0.66	0				Elution from: 37.20 to 37.97 period: A_Noor_211217...	2897000
☑	1.0	(K)LVTMGNPITIFQER(D)	100%	28.1	25.0	28.1	2		538.64	1,612.89	3	67	-0.00016	80	-0.098	0				Elution from: 37.23 to 37.90 period: A_Noor_211217...	1840000
☑	1.0	(K)LVTMGNPITIFQER(D)	97%	14.4	25.0	14.4	2		538.64	1,612.89	3	67	-0.00016	80	-0.098	0				Elution from: 37.23 to 37.90 period: A_Noor_211217...	3186000
☑	1.0	(K)WGDAGAEYVVESTGVFTTMEK(A)	100%	56.5	25.0	56.5	2	Oxidation (+16)	765.01	2,292.02	3	87	-0.0031	107	-1.4	0				Elution from: 35.79 to 36.37 period: A_Noor_211217...	1037000
☑	1.0	(R)WISAPSADAPMFIMGVMHEK(Y)	100%	72.7	25.0	72.7	2	Oxidation (+16), Oxidation (+16)	749.04	2,244.09	3	119	-0.0037	139	-1.7	0				Elution from: 27.96 to 28.70 period: A_Noor_211217...	2716000
☑	1.0	(R)WISAPSADAPMFIMGVMHEK(Y)	100%	69.2	25.0	50.6	2	Oxidation (+16), Oxidation (+16)	749.04	2,244.09	3	119	-0.0037	139	-1.7	0				Elution from: 27.96 to 28.70 period: A_Noor_211217...	2629000
☑	1.0	(R)WISAPSADAPMFIMGVMHEK(Y)	100%	54.2	25.0	17.1	2	Oxidation (+16)	743.71	2,228.10	3	119	0.00043	139	0.19	0				Elution from: 30.43 to 32.14 period: A_Noor_211217...	1120000
☑	1.0	(R)WISAPSADAPMFIMGVMHEK(Y)	100%	78.9	25.0	10.8	2	Oxidation (+16)	743.71	2,228.10	3	119	0.00036	139	0.16	0				Elution from: 30.43 to 32.14 period: A_Noor_211217...	1631000
☑	1.0	(K)IISNASCTTNCLAPLAK(Y)	100%	102.9	25.0	102.9	2	Carbamidomethyl (+57), Carbamidomethyl (+57)	917.46	1,832.91	2	146	-0.0014	162	-0.74	0				Elution from: 26.39 to 26.78 period: A_Noor_211217...	1365000
☑	1.0	(K)VIHDNFGIVEGLMTTVHAITATQK(T)	100%	60.2	25.0	60.2	2	Oxidation (+16)	653.59	2,610.35	4	163	0.000043	186	0.016	0				Elution from: 39.94 to 41.05 period: A_Noor_211217...	3502000
☑	1.0	(K)VIHDNFGIVEGLMTTVHAITATQK(T)	100%	81.6	25.0	81.6	2	Oxidation (+16)	871.12	2,610.35	3	163	-0.0026	186	-1.0	0				Elution from: 40.24 to 40.93 period: A_Noor_211217...	457900
☑	1.0	(K)VIHDNFGIVEGLMTTVHAITATQK(T)	100%	51.2	25.0	51.2	2	Oxidation (+16)	871.12	2,610.35	3	163	-0.0026	186	-1.0	0				Elution from: 40.24 to 40.93 period: A_Noor_211217...	670700
☑	1.0	(K)VIHDNFGIVEGLMTTVHAITATQK(T)	100%	100.1	25.0	100.1	2	Oxidation (+16)	653.59	2,610.35	4	163	0.000043	186	0.016	0				Elution from: 39.94 to 41.05 period: A_Noor_211217...	3049000
☑	1.0	(R)GALQNIIPASTGAAK(A)	100%	41.3	25.0	41.3	2		706.40	1,410.78	2	201	-0.0030	215	-2.1	0				Elution from: 28.36 to 29.24 period: A_Noor_211217...	9314000
☑	1.0	(R)GALQNIIPASTGAAK(A)	100%	27.2	25.0	27.2	2		706.40	1,410.78	2	201	-0.0030	215	-2.1	0				Elution from: 28.36 to 29.24 period: A_Noor_211217...	2791000
☑	1.0	(K)VIPELNGK(L)	99%	29.4	25.0	24.7	2		435.26	868.50	2	220	0.00017	227	0.20	0				Elution from: 22.16 to 22.82 period: A_Noor_211217...	2.151E7
☑	1.0	(R)VPTANYSIVDLTCR(L)	100%	86.3	25.0	81.0	2	Carbamidomethyl (+57)	765.90	1,529.79	2	235	-0.0013	248	-0.86	0				Elution from: 29.18 to 29.76 period: A_Noor_211217...	1503000
☑	1.0	(R)VPTANYSIVDLTCR(L)	100%	96.3	25.0	90.2	2	Carbamidomethyl (+57)	765.90	1,529.79	2	235	-0.0013	248	-0.86	0				Elution from: 29.18 to 29.76 period: A_Noor_211217...	3612000
☑	1.0	(R)VPTANYSIVDLTCR(L)	100%	22.9	25.0	22.9	2	Carbamidomethyl (+57)	510.94	1,529.79	3	235	0.00050	248	0.33	0				Elution from: 29.21 to 29.67 period: A_Noor_211217...	1667000
☑	1.0	(K)QASEGPLK(G)	99%	54.5	25.0	46.2	2		415.22	828.43	2	264	-0.00046	271	-0.56	0				Elution from: 13.56 to 14.98 period: A_Noor_211217...	5366000
☑	1.0	(K)QASEGPLK(G)	99%	42.1	25.0	37.1	2		415.22	828.43	2	264	-0.00046	271	-0.56	0				Elution from: 13.56 to 14.98 period: A_Noor_211217...	1446000
☑	1.0	(K)QASEGPLK(G)	99%	32.7	25.0	20.8	2		415.22	828.43	2	264	-0.00046	271	-0.56	0				Elution from: 13.56 to 15.01 period: A_Noor_211217...	725100
☑	1.0	(K)LISWYDNEFGYSNR(Y)	100%	61.1	25.0	61.1	2		882.40	1,762.79	2	310	-0.00093	323	-0.53	0				Elution from: 34.84 to 35.57 period: A_Noor_211217...	1172000
☑	1.0	(K)LISWYDNEFGYSNR(Y)	100%	86.1	25.0	86.1	2		882.40	1,762.79	2	310	-0.00093	323	-0.53	0				Elution from: 34.84 to 35.57 period: A_Noor_211217...	3219000
☑	1.0	(K)LISWYDNEFGYSNR(Y)	98%	17.8	25.0	17.8	2		588.61	1,762.79	3	310	-0.0013	323	-0.72	0				Elution from: 34.96 to 35.51 period: A_Noor_211217...	1187000
☑	1.0	(R)WDLMAHMASK(-)	100%	50.0	25.0	47.7	2	Oxidation (+16), Oxidation (+16)	617.30	1,232.59	2	324	-0.00066	334	-0.54	0				Elution from: 15.74 to 16.56 period: A_Noor_211217...	785400
☑	1.0	(R)WDLMAHMASK(-)	100%	26.7	25.0	26.7	2	Oxidation (+16), Oxidation (+16)	411.87	1,232.59	3	324	-0.000082	334	-0.066	0				Elution from: 15.65 to 16.31 period: A_Noor_211217...	5870000
☑	1.0	(R)WDLMAHMASK(-)	99%	21.1	25.0	21.1	2	Oxidation (+16), Oxidation (+16)	411.87	1,232.59	3	324	-0.000082	334	-0.066	0				Elution from: 15.65 to 16.31 period: A_Noor_211217...	3698000
☑	1.0	(R)WDLMAHMASKE(-)	100%	33.8	25.0	32.1	2	Oxidation (+16), Oxidation (+16)	681.82	1,361.63	2	324	-0.00055	335	-0.40	0				Elution from: 16.34 to 17.01 period: A_Noor_211217...	392500
☑	1.0	(R)WDLMAHMASKE(-)	100%	28.2	25.0	28.2	2	Oxidation (+16), Oxidation (+16)	454.88	1,361.63	3	324	-0.00065	335	-0.48	0				Elution from: 16.28 to 17.04 period: A_Noor_211217...	4606000

***Figure 4.5**: The figure depicts the probability of G3P protein.*

Sequence Coverage	Protein	Accession	Category	MS/MS Sample	Bio Sample	Prob	%Spec	#Pep	#Uni...	#Spec	%Cov	m.w.
	Glyceraldeh...	G3P_HUMAN	10	A_Noor_211217_020318_10.msm (F082604)	A_Noor_211217_Human_10	100%	0.16%	12	18	31	50%	36 kDa
	Glyceraldeh...	G3P_HUMAN	09	A_Noor_211217_020318_09.msm (F082603)	A_Noor_211217_Human_09	100%	0.046%	7	7	9	33%	36 kDa
	Glyceraldeh...	G3P_HUMAN	08	A_Noor_211217_020318_08.msm (F082602)	A_Noor_211217_Human_08	100%	0.042%	6	7	8	25%	36 kDa
	Glyceraldeh...	G3P_HUMAN	07	A_Noor_211217_020318_07.msm (F082601)	A_Noor_211217_Human_07	100%	0.051%	8	8	10	33%	36 kDa
	Glyceraldeh...	G3P_HUMAN	06	A_Noor_211217_020318_06.msm (F082600)	A_Noor_211217_Human_06	100%	0.031%	6	6	6	23%	36 kDa
	Glyceraldeh...	G3P_HUMAN	05	A_Noor_211217_020318_05.msm (F082599)	A_Noor_211217_Human_05	100%	0.059%	9	9	11	36%	36 kDa
	Glyceraldeh...	G3P_HUMAN	04	A_Noor_211217_020318_04.msm (F082598)	A_Noor_211217_Human_04	100%	0.054%	9	9	10	39%	36 kDa
	Glyceraldeh...	G3P_HUMAN	03	A_Noor_211217_020318_03.msm (F082597)	A_Noor_211217_Human_03	100%	0.097%	14	15	18	48%	36 kDa
	Glyceraldeh...	G3P_HUMAN	02	A_Noor_211217_020318_02-2.msm (F082596)	A_Noor_211217_Human_02...	100%	0.032%	6	6	6	26%	36 kDa
	Glyceraldeh...	G3P_HUMAN	01	A_Noor_211217_020318_01.msm (F082594)	A_Noor_211217_Human_01	100%	0.037%	6	6	7	26%	36 kDa

***Figure 4.6:** Yellow portion in figure shows the sequence coverage of G3P protein.*

A graphical representation of sample spectrum produced by Mass Spectrometry. This is. The peptide data were searched against the UniprotKB homo sapiens reference proteome using the MS/MS ion search engine. b- ions are numbered from left to right on the N-terminus and y-ions are numbered from right to left on the C- terminus.

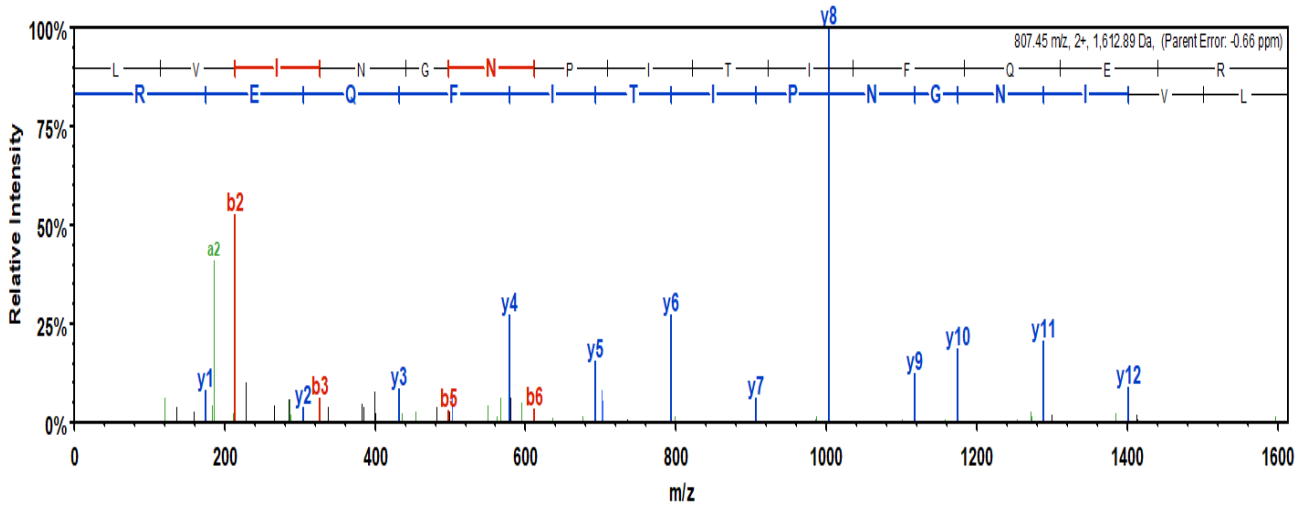

Figure 4.7 *: The above figure illustrates the mass spectrum of G3P protein which shows the mass to charge ratio on the x-axis and relative eintensity on the y-axis*

It displays the same information as the above spectrum in a spreadsheet format. Here the potential ions which match the spectrum are coloured. Red boxes show the b ions while Blue ions show the Y ions and Green boxes refer to the neutral loss or similar fragmentation patterns.

B	B Ions	B+2H	B-NH3	B-H2O	AA	Y Ions	Y+2H	Y-NH3	Y-H2O	Y
1	114.1				L	1,613.9	807.5	1,596.9	1,595.9	14
2	213.2				V	1,500.8	750.9	1,483.8	1,482.8	13
3	326.2				I	1,401.7	701.4	1,384.7	1,383.7	12
4	440.3		423.3		N	1,288.7	644.8	1,271.6	1,270.7	11
5	497.3		480.3		G	1,174.6	587.8	1,157.6	1,156.6	10
6	611.4	306.2	594.3		N	1,117.6	559.3	1,100.6	1,099.6	9
7	708.4	354.7	691.4		P	1,003.6	502.3	986.5	985.5	8
8	821.5	411.2	804.5		I	906.5	453.8	889.5	888.5	7
9	922.5	461.8	905.5	904.5	T	793.4	397.2	776.4	775.4	6
10	1,035.6	518.3	1,018.6	1,017.6	I	692.4		675.3	674.4	5
11	1,182.7	591.8	1,165.7	1,164.7	F	579.3		562.3	561.3	4
12	1,310.7	655.9	1,293.7	1,292.7	Q	432.2		415.2	414.2	3
13	1,439.8	720.4	1,422.8	1,421.8	E	304.2		287.1	286.2	2
14	1,613.9	807.5	1,596.9	1,595.9	R	175.1		158.1		1

Figure 4.8: *The figure shows the fragmentation table*

The glycolytic enzyme that catalyzes the conversion of 2-phosphoglycerate to phosphoenolpyruvate is Alpha Enolase. It is involved in various processes such as growth control allergic responses in addition to glycolysis. Alzheimer and Cancer Associated Retinopathy Diseases are associated with ENO1 . Among its related pathways are Glucose metabolism.

The exported raw MS/MS data of ENOA protein obtained from the Scaffold database. It shows that ENOA protein was obtained from homo sapiens with a molecular weight of 47,170.2Da. There were 18 exclusive unique peptides including 21 exclusive unique spectra,34 total spectra were identified with an amino acid of 251 out of 434 and with a 58% coverage. Amino acids that matched MS/MS spectra are in yellow.

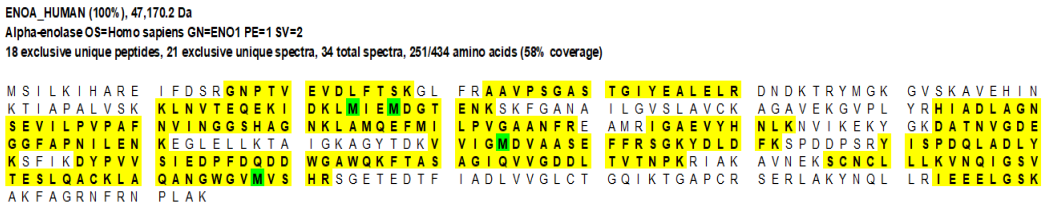

Figure 4.9 *:The identified peptides of the ENOA protein is shown in figure.*

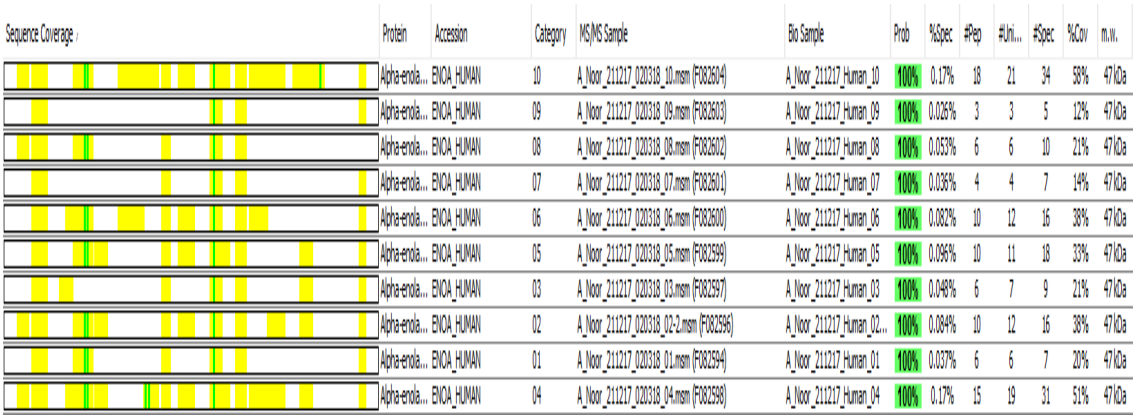

Sequence Coverage	Protein	Accession	Category	MS/MS Sample	Bio Sample	Prob	%Spec	#Pep	#Un...	#Spec	%Cov	m.w.
	Alpha-enola...	ENOA_HUMAN	10	A_Noor_211217_020318_10.msm (F082604)	A_Noor_211217_Human_10	100%	0.17%	18	21	34	58%	47kDa
	Alpha-enola...	ENOA_HUMAN	09	A_Noor_211217_020318_09.msm (F082603)	A_Noor_211217_Human_09	100%	0.026%	3	3	5	12%	47kDa
	Alpha-enola...	ENOA_HUMAN	08	A_Noor_211217_020318_08.msm (F082602)	A_Noor_211217_Human_08	100%	0.053%	6	6	10	21%	47kDa
	Alpha-enola...	ENOA_HUMAN	07	A_Noor_211217_020318_07.msm (F082601)	A_Noor_211217_Human_07	100%	0.036%	4	4	7	14%	47kDa
	Alpha-enola...	ENOA_HUMAN	06	A_Noor_211217_020318_06.msm (F082600)	A_Noor_211217_Human_06	100%	0.082%	10	12	16	38%	47kDa
	Alpha-enola...	ENOA_HUMAN	05	A_Noor_211217_020318_05.msm (F082599)	A_Noor_211217_Human_05	100%	0.096%	10	11	18	33%	47kDa
	Alpha-enola...	ENOA_HUMAN	03	A_Noor_211217_020318_03.msm (F082597)	A_Noor_211217_Human_03	100%	0.048%	6	7	9	21%	47kDa
	Alpha-enola...	ENOA_HUMAN	02	A_Noor_211217_020318_02-2.msm (F082596)	A_Noor_211217_Human_02...	100%	0.084%	10	12	16	38%	47kDa
	Alpha-enola...	ENOA_HUMAN	01	A_Noor_211217_020318_01.msm (F082594)	A_Noor_211217_Human_01	100%	0.037%	6	6	7	20%	47kDa
	Alpha-enola...	ENOA_HUMAN	04	A_Noor_211217_020318_04.msm (F082598)	A_Noor_211217_Human_04	100%	0.17%	15	19	31	51%	47kDa

Figure 4.10: *The figure depicts the probability and sequence coverage of ENOA protein.*

A graphical representation of sample spectrum produced by Mass Spectrometry. This is a simplified mass spectrum of ENOA protein which shows the mass to charge ratio on the x-axis and relative intensity on the y-axis. The peptide data were searched against the UniprotKB homo sapiens reference proteome using the MS/MS ion search engine. In the above graph, b- ions are numbered from left to right on the N-terminus and y-ions are numbered from right to left on the C- terminus.

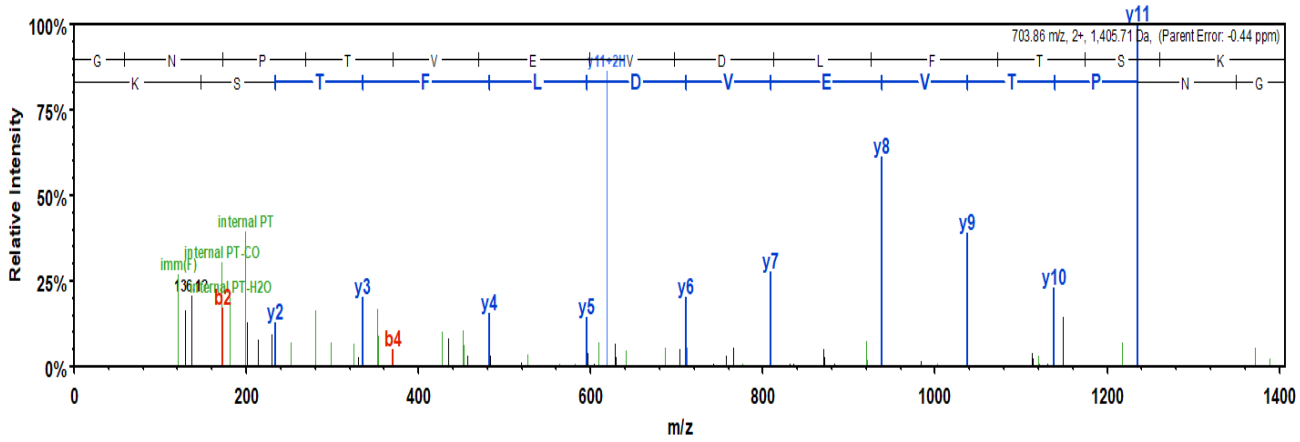

Figure 4.11: *The figure represents mass spectrum of ENOA protein.*

The table displays the same information as the above spectrum in a spreadsheet format. Here the potential ions which match the spectrum are coloured. Red boxes show the b ions while Blue ions show the Y ions and Green boxes refer to the neutral loss or similar fragmentation patterns.

B	B Ions	B+2H	B-NH3	B-H2O	AA	Y Ions	Y+2H	Y-NH3	Y-H2O	Y
1	58.0				G	1,406.7	703.9	1,389.7	1,388.7	13
2	172.1		155.0		N	1,349.7	675.4	1,332.7	1,331.7	12
3	269.1		252.1		P	1,235.7	618.3	1,218.6	1,217.6	11
4	370.2		353.1	352.2	T	1,138.6	569.8	1,121.6	1,120.6	10
5	469.2		452.2	451.2	V	1,037.6	519.3	1,020.5	1,019.5	9
6	598.3	299.6	581.3	580.3	E	938.5	469.7	921.5	920.5	8
7	697.4	349.2	680.3	679.3	V	809.4	405.2	792.4	791.4	7
8	812.4	406.7	795.4	794.4	D	710.4	355.7	693.3	692.4	6
9	925.5	463.2	908.4	907.5	L	595.3		578.3	577.3	5
10	1,072.5	536.8	1,055.5	1,054.5	F	482.3		465.2	464.3	4
11	1,173.6	587.3	1,156.6	1,155.6	T	335.2		318.2	317.2	3
12	1,260.6	630.8	1,243.6	1,242.6	S	234.1		217.1	216.1	2
13	1,406.7	703.9	1,389.7	1,388.7	K	147.1		130.1		1

Figure 4.12: *The fragmentation table of ENOA is shown in figure.*

The gene belongs to the angiotensin-converting enzyme family of dipeptidyl carboxydipeptidases and has considerable homology to human angiotensin 1 converting enzyme is pyruvate kinase.The cleavage of angiotensin I into angiotensin 1-9, and angiotensin II into the vasodilator angiotensin 1-7 is catalyzed by this secreted protein.The regulation of cardiovascular and renal function, as well as fertility suggested by the organ and cell specific expression of this gene is the role played by this protein.

The exported raw MS/MS data of Pyruvate kinase protein obtained from the Scaffold database. This shows the identified peptides of the ENOA protein.The protein was obtained from homo sapiens with a molecular weight of 457,937.5Da. There were 11 exclusive unique peptides including 12 exclusive unique spectra,34 total spectra were identified with an amino acid of 154 out of 531 and with a 29% coverage. Amino acids that matched MS/MS spectra are in yellow.

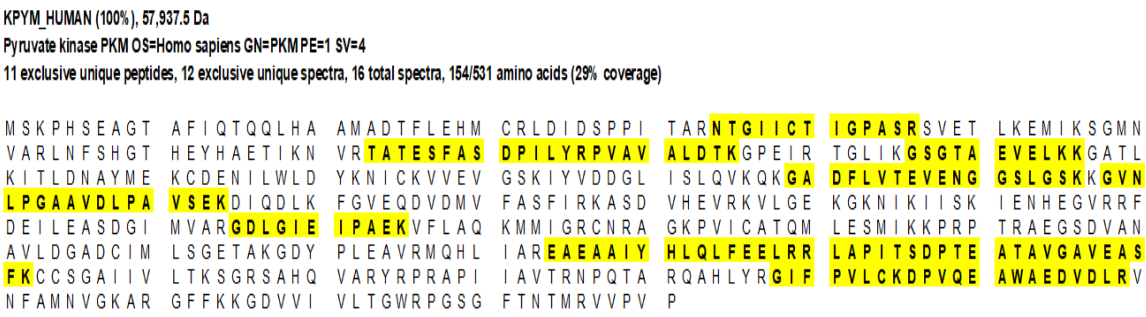

Figure 4.13: *The figure illustrates the unique peptides of pyruvate kinase.*

Valid	Weight	Sequence	Prob	Mascot Ion score	Masc...	Masc...	NTT	Modifications	Observed	Actual Mass	Charge	Start	Delta Da	Stop	Delta PPM	# Ot...	Rete...	Other Prot...	Intensity	Spectrum ID	TIC
☐	1.0	(R)GNPTVEVDLPTSK(G)	100%	74.5	25.0	23.7	2		703.86	1,405.71	2	16	-0.00061	28	-0.44	0				Elution from: 31.74 to 32.42 period: A_Noor_211217...	1666000
☐	1.0	(R)GNPTVEVDLPTSK(G)	100%	74.7	25.0	23.3	2		703.86	1,405.71	2	16	-0.00061	28	-0.44	0				Elution from: 31.74 to 32.42 period: A_Noor_211217...	3677000
☐	0.6	(R)AAYPSGASTGIYEALELR(D)	100%	100.0	25.0	100.0	2		602.32	1,803.94	3	33	0.00063	50	0.35	1		ENOG_HUMAN		Elution from: 35.30 to 36.28 period: A_Noor_211217...	2414000
☐	0.6	(R)AAYPSGASTGIYEALELR(D)	100%	118.1	25.0	116.7	2		902.98	1,803.94	2	33	-0.00066	50	-0.37	1		ENOG_HUMAN		Elution from: 35.39 to 36.00 period: A_Noor_211217...	3216000
☐	0.6	(R)AAYPSGASTGIYEALELR(D)	100%	121.1	25.0	119.1	2		902.98	1,803.94	2	33	-0.00066	50	-0.37	1		ENOG_HUMAN		Elution from: 35.39 to 36.00 period: A_Noor_211217...	1377000
☐	1.0	(K)LNVTEQEK(I)	100%	62.8	25.0	34.7	2		544.80	1,087.59	2	81	-0.00020	89	-0.18	0				Elution from: 13.10 to 13.99 period: A_Noor_211217...	790000
☐	1.0	(K)LNVTEQEK(I)	100%	52.0	25.0	26.7	2		544.80	1,087.59	2	81	-0.00020	89	-0.18	0				Elution from: 13.10 to 13.59 period: A_Noor_211217...	411980
☐	1.0	(K)LNVTEQEK(I)	99%	32.5	25.0	8.8	2		363.54	1,087.59	3	81	-0.00038	89	-0.35	0				Elution from: 13.07 to 14.06 period: A_Noor_211217...	4344000
☐	1.0	(K)LNVTEQEK(I)	99%	41.1	25.0	29.2	2		480.75	959.49	2	82	0.00093	89	0.97	0				Elution from: 15.50 to 16.11 period: A_Noor_211217...	851200
☐	1.0	(K)LNVTEQEK(I)	99%	33.7	25.0	22.2	2		480.75	959.49	2	82	0.00093	89	0.97	0				Elution from: 15.50 to 16.11 period: A_Noor_211217...	640300
☐	1.0	(K)IDKLMIEMDGTENK(S)	100%	69.2	25.0	69.2	2	Oxidation (+16), Oxidation (+16)	556.93	1,667.77	3	90	-0.00084	103	-0.51	0				Elution from: 20.32 to 20.84 period: A_Noor_211217...	1488000
☐	1.0	(K)IDKLMIEMDGTENK(S)	100%	54.3	25.0	54.3	2	Oxidation (+16), Oxidation (+16)	834.89	1,667.77	2	90	-0.0031	103	-1.9	0				Elution from: 20.41 to 20.72 period: A_Noor_211217...	371800
☐	1.0	(K)LMIEMDGTENK(S)	100%	51.2	25.0	51.2	2	Oxidation (+16), Oxidation (+16)	656.79	1,311.57	2	93	-0.00049	103	-0.38	0				Elution from: 18.52 to 19.15 period: A_Noor_211217...	1507000
☐	1.0	(R)HADLKGNSEVILPVPAFNVINGGSHAGNKIL)	100%	72.3	25.0	72.3	2		753.65	3,010.56	4	133	0.0016	162	0.54	0				Elution from: 37.14 to 38.06 period: A_Noor_211217...	3959000
☐	1.0	(R)HADLKGNSEVILPVPAFNVINGGSHAGNKIL)	100%	58.0	25.0	58.0	2		753.65	3,010.56	4	133	0.0016	162	0.54	0				Elution from: 37.14 to 38.06 period: A_Noor_211217...	1635000
☐	1.0	(R)HADLKGNSEVILPVPAFNVINGGSHAGNKIL)	100%	32.7	25.0	32.7	2		753.65	3,010.56	4	133	0.0016	162	0.54	0				Elution from: 37.14 to 38.06 period: A_Noor_211217...	2697000
☐	1.0	(K)LAMQEPMILPVGAANPI(E)	98%	15.6	25.0	15.6	2		954.50	1,906.98	2	163	0.00063	179	0.33	0				Elution from: 42.87 to 43.22 period: A_Noor_211217...	98930
☐	1.0	(R)SAEVYHNK(N)	100%	60.2	25.0	47.8	2		572.31	1,142.61	2	184	-0.0016	193	-1.4	0				Elution from: 19.93 to 20.75 period: A_Noor_211217...	1427000
☐	1.0	(K)DATNYGDESGFNPNLENK(E)	100%	103.8	25.0	103.8	2		980.96	1,959.92	2	203	-0.0023	221	-1.2	0				Elution from: 31.62 to 32.17 period: A_Noor_211217...	1230000
☐	1.0	(K)DATNYGDESGFNPNLENK(E)	100%	111.2	25.0	111.2	2		980.96	1,959.92	2	203	-0.0023	221	-1.2	0				Elution from: 31.62 to 32.17 period: A_Noor_211217...	761800
☐	1.0	(K)VIYG*IDVAASEFFR(S)	100%	72.5	25.0	72.5	2	Oxidation (+16)	778.89	1,555.77	2	240	-0.0010	253	-0.65	0				Elution from: 34.96 to 35.57 period: A_Noor_211217...	1577000
☐	1.0	(K)VIYG*IDVAASEFFR(S)	100%	72.8	25.0	72.8	2	Oxidation (+16)	778.89	1,555.77	2	240	-0.0010	253	-0.65	0				Elution from: 34.96 to 35.57 period: A_Noor_211217...	1791000
☐	1.0	(R)SGKYDLDFK(S)	100%	28.7	25.0	28.7	2		358.18	1,071.52	3	254	-0.00032	262	-0.30	0				Elution from: 23.46 to 23.91 period: A_Noor_211217...	2092000
☐	1.0	(R)YISPDQLADLYK(S)	100%	63.7	25.0	63.7	2		713.37	1,424.72	2	270	-0.0010	281	-0.70	0				Elution from: 33.79 to 34.50 period: A_Noor_211217...	1555000
☐	1.0	(R)YISPDQLADLYK(S)	100%	86.6	25.0	86.6	2		713.37	1,424.72	2	270	-0.0010	281	-0.70	0				Elution from: 33.79 to 34.50 period: A_Noor_211217...	1.11E7
☐	1.0	(K)DYPVVSIEDPFDQDDWGAWQK(F)	100%	59.7	25.0	59.7	2		837.38	2,509.11	3	286	-0.0020	306	-0.78	0				Elution from: 41.61 to 42.13 period: A_Noor_211217...	637900
☐	1.0	(K)DYPVVSIEDPFDQDDWGAWQK(F)	100%	48.6	25.0	48.6	2		1,255.56	2,509.11	2	286	0.0026	306	1.0	0				Elution from: 41.73 to 42.04 period: A_Noor_211217...	331700
☐	1.0	(K)DYPVVSIEDPFDQDDWGAWQK(F)	100%	93.2	25.0	93.2	2		837.38	2,509.11	3	286	-0.0020	306	-0.78	0				Elution from: 41.61 to 42.13 period: A_Noor_211217...	1418000
☐	1.0	(K)FTASAGIQVVGDDLTVTNPK(R)	100%	65.6	25.0	65.6	2		678.36	2,032.05	3	307	0.0019	326	0.95	0				Elution from: 32.60 to 33.43 period: A_Noor_211217...	1369000
☐	1.0	(K)SCNCLLKV(Y)	99%	36.5	25.0	19.0	2	Carbamidomethyl (+57), Carbamidomethyl (+57)	504.25	1,006.49	2	336	0.00046	343	0.46	0				Elution from: 24.28 to 25.58 period: A_Noor_211217...	3903000
☐	1.0	(K)VNQJQSVTESLQACK(L)	100%	102.9	25.0	0.0	2	Carbamidomethyl (+57)	817.41	1,632.81	2	344	-0.0010	358	-0.64	0				Elution from: 26.51 to 27.02 period: A_Noor_211217...	1626000
☐	1.0	(K)VNQJQSVTESLQACK(L)	100%	111.0	25.0	0.0	2	Carbamidomethyl (+57)	817.41	1,632.81	2	344	-0.0010	358	-0.64	0				Elution from: 26.51 to 27.02 period: A_Noor_211217...	1311000
☐	1.0	(K)LAQANGWGMYMSHR(S)	100%	37.5	25.0	37.5	2	Oxidation (+16)	514.59	1,540.76	3	359	0.0026	372	1.7	0				Elution from: 23.27 to 23.76 period: A_Noor_211217...	2604000
☐	1.0	(R)EEELQSK(A)	99%	39.5	25.0	12.2	2		452.73	903.45	2	413	-0.0018	420	-2.0	0				Elution from: 16.46 to 17.71 period: A_Noor_211217...	2294000

Figure 4.14: *This figure depicts the probability and sequence coverage of KPYM protein.*

This is a simplified mass spectrum of KPYM protein which shows the mass to charge ratio on the x-axis and relative intensity on the y-axis. The peptide data were searched against the UniprotKB homo sapiens reference proteome using the MS/MS ion search engine. In the above graph, b- ions are numbered from left to right on the N-terminus and y-ions are numbered from right to left on the C- terminus.

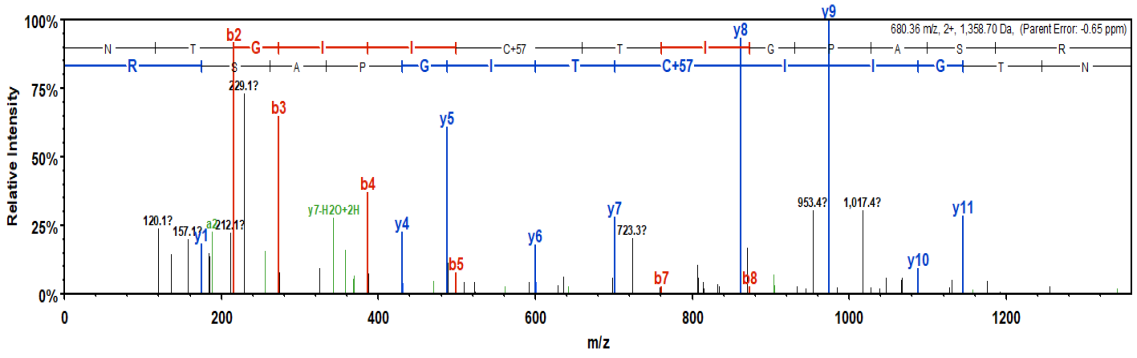

Figure 4.15: *The figure illustrates sample spectrum produced by Mass Spectrometry.*

B	B Ions	B+2H	B-NH3	B-H2O	AA	Y Ions	Y+2H	Y-NH3	Y-H2O	Y
1	115.1		98.0		N	1,359.7	680.4	1,342.7	1,341.7	13
2	216.1		199.1	198.1	T	1,245.7	623.3	1,228.6	1,227.7	12
3	273.1		256.1	255.1	G	1,144.6	572.8	1,127.6	1,126.6	11
4	386.2		369.2	368.2	I	1,087.6	544.3	1,070.6	1,069.6	10
5	499.3		482.3	481.3	I	974.5	487.8	957.5	956.5	9
6	659.3	330.2	642.3	641.3	C+57	861.4	431.2	844.4	843.4	8
7	760.4	380.7	743.3	742.4	T	701.4	351.2	684.4	683.4	7
8	873.5	437.2	856.4	855.4	I	600.3	300.7	583.3	582.3	6
9	930.5	465.7	913.4	912.5	G	487.3		470.2	469.3	5
10	1,027.5	514.3	1,010.5	1,009.5	P	430.2		413.2	412.2	4
11	1,098.6	549.8	1,081.5	1,080.6	A	333.2		316.2	315.2	3
12	1,185.6	593.3	1,168.6	1,167.6	S	262.2		245.1	244.1	2
13	1,359.7	680.4	1,342.7	1,341.7	R	175.1		158.1		1

Figure 4.16: *The figure shows fragmentation table.*

It displays the same information as the above spectrum in a spreadsheet format. Here the potential ions which match the spectrum are coloured. Red boxes show the b ions while Blue ions show the Y ions and Green boxes refer to the neutral loss or similar fragmentation patterns.

Valid	Weight	Sequence	Prob	Mascot Ion score	Masc...	Masc...	NTT	Modifications	Observed	Actual Mass	Charge	Start	Delta
☑	1.0	(R)NTGIICTIGPASR(S)	100%	57.7	25.0	46.4	2	Carbamidomethyl (+57)	680.36	1,358.70	2	44	
☑	1.0	(R)TATESFASDPILYRPVAVALDTK(G)	100%	67.5	25.0	67.5	2		822.44	2,464.29	3	93	
☑	1.0	(R)TATESFASDPILYRPVAVALDTK(G)	100%	91.8	25.0	91.8	2		822.44	2,464.29	3	93	
☑	1.0	(K)GSGTAEVELK(K)	100%	53.4	25.0	45.6	2		495.76	989.50	2	126	
☑	1.0	(K)GSGTAEVELKK(G)	100%	37.3	25.0	35.8	2		373.54	1,117.60	3	126	
☑	1.0	(K)GADFLVTEVENGGSLGSK(K)	100%	56.6	25.0	49.8	2		890.44	1,778.87	2	189	
☑	1.0	(K)GADFLVTEVENGGSLGSK(K)	100%	36.6	25.0	36.6	2		890.44	1,778.87	2	189	
☑	1.0	(K)GVNLPGAAVDLPAVSEK(D)	100%	54.1	25.0	54.1	2		818.95	1,635.89	2	208	
☑	0.9	(R)GDLGIEIPAEK(V)	100%	43.5	25.0	32.7	2		571.31	1,140.60	2	338	
☑	1.0	(R)EAEAAIYHLQLFEELRR(L)	100%	22.7	25.0	22.7	2		522.78	2,087.08	4	384	
☑	1.0	(R)LAPITSDPTEATAVGAVEASFK(C)	100%	53.9	25.0	53.9	2		725.71	2,174.11	3	401	
☑	1.0	(R)LAPITSDPTEATAVGAVEASFK(C)	100%	39.6	25.0	39.6	2		725.71	2,174.11	3	401	
☑	1.0	(R)LAPITSDPTEATAVGAVEASFK(C)	100%	117.9	25.0	117.9	2		1,088.06	2,174.11	2	401	
☑	1.0	(R)GIFPVLCK(D)	99%	32.3	25.0	18.9	2	Carbamidomethyl (+57)	467.27	932.52	2	468	
☑	1.0	(R)GIFPVLCKDPVQEAWAEDVDLR(V)	100%	65.4	25.0	65.4	2	Carbamidomethyl (+57)	853.10	2,556.27	3	468	
☑	1.0	(K)DPVQEAWAEDVDLR(V)	100%	74.9	25.0	74.9	2		821.89	1,641.76	2	476	

Figure 4.17 *: The figure depicts sequence and probability of KPYM protein.*

The reversible oxidation of malate to oxaloacetate, utilizing the NAD/NADH cofactor system in the citric acid cycle is catalyzed by Malate Dehydrogenase cytoplasmic. The protein encoded by this gene is localized to the mitochondria.It play the pivotal roles in the malate-aspartate shuttle that operates in the metabolic coordination between cytosol and mitochondria. The variants encoding different isoforms have been found for this gene in several transcript. The Glucose metabolism and Glyoxylate and dicarboxylate metabolism are among its related pathways.

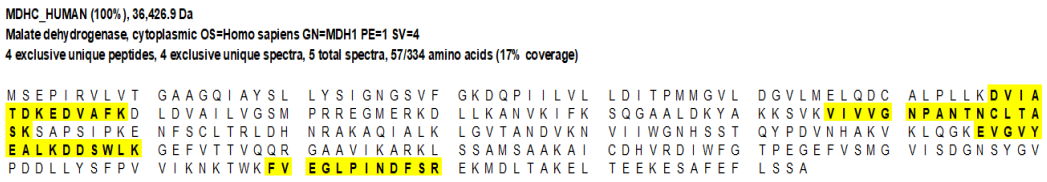
MDHC_HUMAN (100%), 36,426.9 Da
Malate dehydrogenase, cytoplasmic OS=Homo sapiens GN=MDH1 PE=1 SV=4
4 exclusive unique peptides, 4 exclusive unique spectra, 5 total spectra, 57/334 amino acids (17% coverage)

MSEPIRVLVT GAAGQIAYSL LYSIGNGSVF GKDQPIILVL LDITPMMGVL DGVLMELQDC ALPLLKDVIA
TDKEDVAFKD LDVAILVGSM PRREGMERKD LLKANVKIFK SQGAALDKYA KKSVKVIVVG NPANTNCLTA
SKSAPSIPKE NFSCLTRLDH NRAKAQIALK LGVTANDVKN VIIWGNHSST QYPDVNHAKV KLQGKEVGVY
EALKDDSWLK GEFVTTVQQR GAAVIKARKL SSAMSAAKAI CDHVRDIWFG TPEGEFVSMG VISDGNSYGV
PDDLLYSFPV VIKNKTWKFV EGLPINDFSR EKMDLTAKEL TEEKESAFEF LSSA

Figure 4.18 : *The figure demonstrated identified peptides of malate dehydrogenase cytoplasmic protein.*

It shows the exported raw MS/MS data of malate dehydrogenase cytoplasmic protein obtained from the Scaffold database. This shows the identified peptides of the malate dehydrogenase cytoplasmic protein shows that Malate Dehydrogenase protein was obtained from homo sapiens with a molecular weight of 36,426.9Da. There were 4 exclusive unique peptides, from which 4 exclusive unique spectra were identified with an amino acid of 57 out of 334 and with a 17% coverage. Amino acids that matched MS/MS spectra are in yellow. It shows the probability and sequence coverage of MDHC protein.

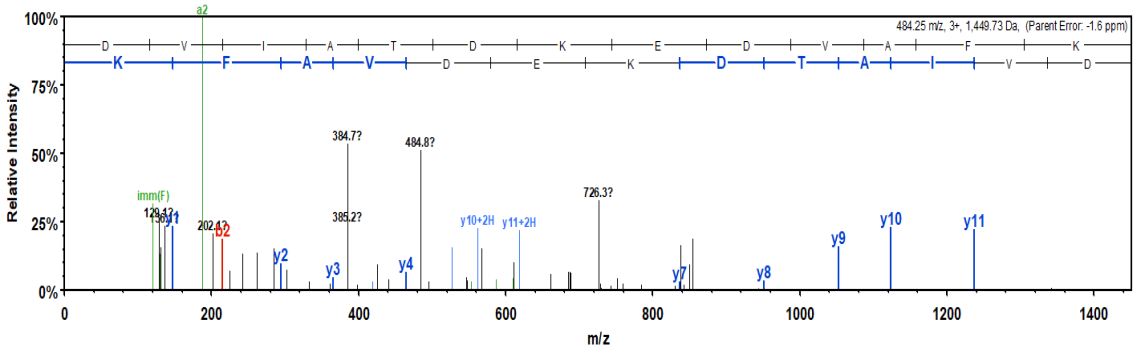

Figure 4.19: *The figure shows graphical representation of sample spectrum produced by Mass Spectrometry.*

This is a simplified mass spectrum of MDHC protein which shows the mass to charge ratio on the x-axis and relative intensity on the y-axis. The peptide data were searched against the UniprotKB homo sapiens reference proteome using the MS/MS ion search engine. In the above graph, b- ions are numbered from left to right on the N-terminus and y-ions are numbered from right to left on the C- terminus**.**

Valid	Weight	Sequence	Prob	Mascot Ion score	Masc...	Masc...	NTT	Modifications
☑	1.0	(K)DVIATDKEDVAFK(D)	100%	28.1	25.0	28.1	2	
☑	1.0	(K)VIVVGNPANTNCLTASK(S)	100%	86.7	25.0	86.7	2	Carbamidomethyl (+57
☑	1.0	(K)EVGWYEALKDDSWLK(G)	100%	78.2	25.0	78.2	2	
☑	1.0	(K)FVEGLPINDFSR(E)	100%	36.0	25.0	36.0	2	
☑	1.0	(K)FVEGLPINDFSR(E)	100%	25.5	25.0	25.5	2	

Figure 4.20: *The figure shows probability of MDHC protein.*

B	B Ions	B+2H	B-NH3	B-H2O	AA	Y Ions	Y+2H	Y-NH3	Y-H2O	Y
1	116.0	58.5		98.0	D	1,450.7	725.9	1,433.7	1,432.7	13
2	215.1	108.1		197.1	V	1,335.7	668.4	1,318.7	1,317.7	12
3	328.2	164.6		310.2	I	1,236.6	618.8	1,219.6	1,218.6	11
4	399.2	200.1		381.2	A	1,123.6	562.3	1,106.5	1,105.6	10
5	500.3	250.6		482.3	T	1,052.5	526.8	1,035.5	1,034.5	9
6	615.3	308.2		597.3	D	951.5	476.2	934.5	933.5	8
7	743.4	372.2	726.4	725.4	K	836.5	418.7	819.4	818.4	7
8	872.4	436.7	855.4	854.4	E	708.4	354.7	691.3	690.3	6
9	987.5	494.2	970.4	969.5	D	579.3	290.2	562.3	561.3	5
10	1,086.5	543.8	1,069.5	1,068.5	V	464.3	232.6	447.3		4
11	1,157.6	579.3	1,140.5	1,139.6	A	365.2	183.1	348.2		3
12	1,304.6	652.8	1,287.6	1,286.6	F	294.2	147.6	277.2		2
13	1,450.7	725.9	1,433.7	1,432.7	K	147.1	74.1	130.1		1

Figure 4.21: *This is the fragmentation table of MDHC protein.*

It displays the same information as the above spectrum in a spreadsheet format. Here the potential ions which match the spectrum are coloured. Red boxes show the b ions while Blue ions show the Y ions and Green boxes refer to the neutral loss or similar fragmentation patterns.

The exported raw MS/MS data of MDHM protein obtained from the Scaffold database. This shows the identified peptides of the MDHM protein.MDHM protein was obtained from homo sapiens with a molecular weight of 11,676D. There were 9 exclusive unique peptides, from which 9 exclusive unique spectra were identified with an amino acid of 115 out of 338 and with a 34% coverage. Amino acids that matched MS/MS spectra are in yellow.

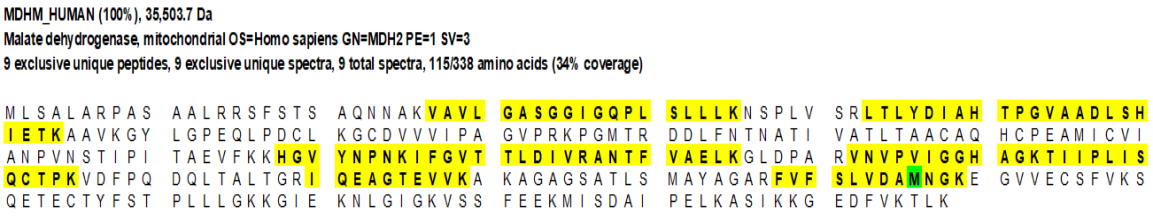

Figure 4.22 : *The figure represents peptides sequences of MDHM protein.*

Valid	Weight	Sequence	Prob	Mascot Ion score	Masc...	Masc...	NTT	Modifications	Observed	Actual Mass	Charge	Start
☑	1.0	(K)VAVLGASGGIGQPLSLLLK(N)	100%	76.6	25.0	76.6	2		897.05	1,792.08	2	27
☑	1.0	(R)LTLYDIAHTPGVAADLSHIETK(A)	100%	108.9	25.0	108.9	2		592.07	2,364.23	4	53
☑	1.0	(K)HGVYNPNK(I)	95%	18.2	25.0	18.2	2		464.73	927.46	2	158
☑	1.0	(K)IFGVTTLDIVR(A)	100%	51.8	25.0	50.0	2		617.36	1,232.71	2	166
☑	1.0	(R)ANTFVAELK(G)	100%	53.0	25.0	48.6	2		496.77	991.53	2	177
☑	1.0	(R)VNVPVIGGHAGK(T)	100%	29.5	25.0	29.5	2		383.22	1,146.65	3	192
☑	1.0	(K)TIIPLISQCTPK(V)	100%	42.4	25.0	41.5	2	Carbamidomethyl (+57)	685.89	1,369.76	2	204
☑	1.0	(R)IQEAGTEVVK(A)	100%	35.6	25.0	26.5	2		537.30	1,072.58	2	230
☑	1.0	(R)FVFSLVDAMNGK(E)	100%	38.7	25.0	38.7	2	Oxidation (+16)	672.34	1,342.66	2	258

Figure 4.23: *The figure shows probability and sequence of MDHM protein.*

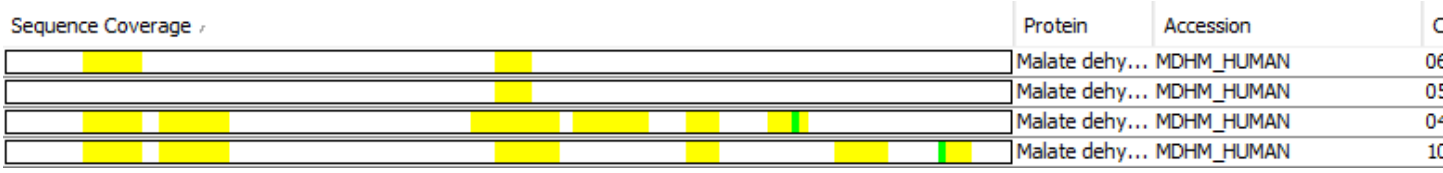

Figure 4.24: *This figure shows the probability and sequence coverage of MDHM protein.*

This is a simplified mass spectrum of MDHM protein which shows the mass to charge ratio on the x-axis and relative intensity on the y-axis. The peptide data were searched against the

UniprotKB homo sapiens reference proteome using the MS/MS ion search engine. In the above graph, b- ions are numbered from left to right on the N-terminus and y-ions are numbered from right to left on the C- terminus.

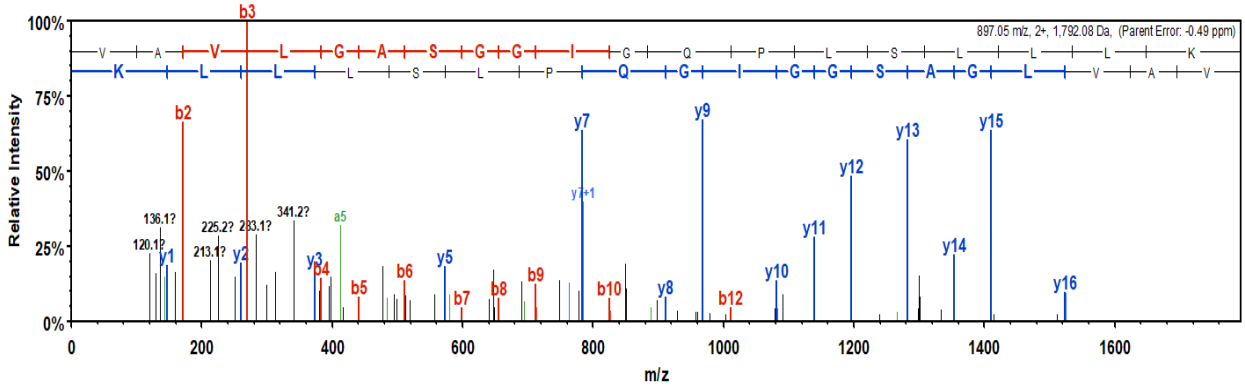

Figure 4.25:*The figure illustrates graphical representation of sample spectrum produced by Mass Spectrometry.*

B	B Ions	B+2H	B-NH3	B-H2O	AA	Y Ions	Y+2H	Y-NH3	Y-H2O	Y
1	100.1				V	1,793.1	897.0	1,776.1	1,775.1	19
2	171.1				A	1,694.0	847.5	1,677.0	1,676.0	18
3	270.2				V	1,623.0	812.0	1,606.0	1,605.0	17
4	383.3				L	1,523.9	762.5	1,506.9	1,505.9	16
5	440.3				G	1,410.8	705.9	1,393.8	1,392.8	15
6	511.3	256.2			A	1,353.8	677.4	1,336.8	1,335.8	14
7	598.4	299.7		580.3	S	1,282.8	641.9	1,265.7	1,264.8	13
8	655.4	328.2		637.4	G	1,195.7	598.4	1,178.7	1,177.7	12
9	712.4	356.7		694.4	G	1,138.7	569.9	1,121.7	1,120.7	11
10	825.5	413.2		807.5	I	1,081.7	541.4	1,064.7	1,063.7	10
11	882.5	441.8		864.5	G	968.6	484.8	951.6	950.6	9
12	1,010.6	505.8	993.5	992.6	Q	911.6	456.3	894.6	893.6	8
13	1,107.6	554.3	1,090.6	1,089.6	P	783.5	392.3	766.5	765.5	7
14	1,220.7	610.9	1,203.7	1,202.7	L	686.5	343.7	669.5	668.5	6
15	1,307.7	654.4	1,290.7	1,289.7	S	573.4		556.4	555.4	5
16	1,420.8	710.9	1,403.8	1,402.8	L	486.4		469.3		4
17	1,533.9	767.5	1,516.9	1,515.9	L	373.3		356.3		3
18	1,647.0	824.0	1,630.0	1,629.0	L	260.2		243.2		2
19	1,793.1	897.0	1,776.1	1,775.1	K	147.1		130.1		1

Figure 4.26: *This figure shows fragmentation table of MDHM protein.*

PGK1_HUMAN (100%), 44,615.3 Da
Phosphoglycerate kinase 1 OS=Homo sapiens GN=PGK1 PE=1 SV=3
3 exclusive unique peptides, 3 exclusive unique spectra, 5 total spectra, 41/417 amino acids (10% coverage)

M S L S N K L T L D K L D V K G K R V V M R V D F N V P M K **N N Q I T N N Q R** I K A A V P S I K F C L D N G A K S V V L M S H L G R P D G V
P M P D K Y S L E P V A V E L K S L L G K D V L F L K D C V G P E V E K A C A N P A A G S V I L L E N L R F H V E E E G K G K D A S G N K V
K A E P A K I E A F R A S L S K **L G D V** **Y V N D A F G T A H** **R** A H S S M V G V N L P Q K A G G F L M K K E L N Y F A K **A** **L E S P E R P F L A**
I L G G A K V A D K I Q L I N N M L D K V N E M I I G G G M A F T F L K V L N N M E I G T S L F D E E G A K I V K D L M S K A E K N G V K I
T L P V D F V T A D K F D E N A K T G Q A T V A S G I P A G W M G L D C G P E S S K K Y A E A V T R A K Q I V W N G P V G V F E W E A F A R
G T K A L M D E V V K A T S R G C I T I I G G G D T A T C C A K W N T E D K V S H V S T G G G A S L E L L E G K V L P G V D A L S N I

Figure 4.27: *The figure illustrated peptides sequences of PGK1protein.*

Valid	Weight	Sequence	Prob	Mascot Ion score	Masc...	Masc...	NTT	M
☑	1.0	(K)NNQITNNQR(I)	100%	51.6	25.0	49.3	2	
☑	1.0	(K)LGDVYVNDAFGTAHR(A)	100%	78.3	25.0	78.3	2	
☑	1.0	(K)ALESPERPFLAILGGAK(V)	100%	69.2	25.0	67.8	2	
☑	1.0	(K)ALESPERPFLAILGGAK(V)	100%	77.0	25.0	77.0	2	
☑	1.0	(K)ALESPERPFLAILGGAK(V)	100%	49.2	25.0	49.2	2	

Figure 4.28: *The figure demonstrates probability of PGK1protein.*

Figure 4.29: *The figure demonstrates sequence coverage of PGK1protein.*

The exported raw MS/MS data of phosphoglycerate kinase protein obtained from the Scaffold database. This shows the identified peptides of the PGK1.PGK1 protein was obtained from homo sapiens with a molecular weight of 44,615.3Da. There were 3 exclusive unique peptides, from which 3 exclusive unique spectra were identified with an amino acid of 41 out of 417 and with a 10% coverage. Amino acids that matched MS/MS spectra are in yellow.

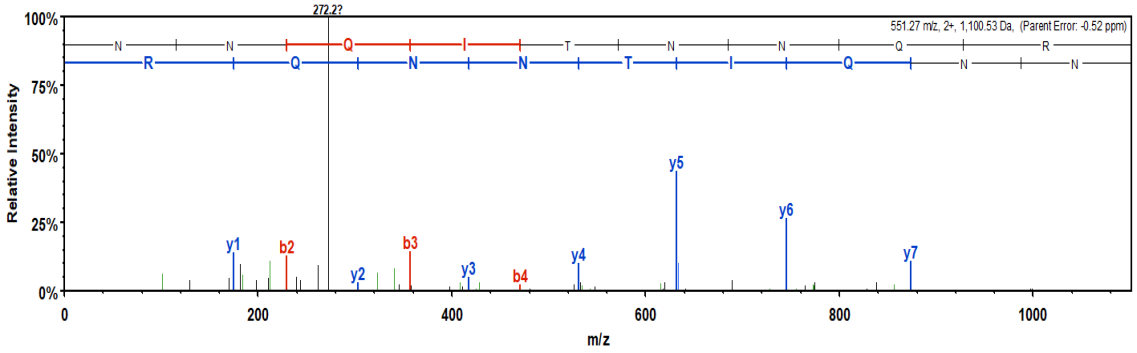

Figure 4.29: *The figures shows mass to charge ratio of PGK1 protein.*

A graphical representation of sample spectrum produced by Mass Spectrometry. This is a simplified mass spectrum of PGK1 protein which shows the mass to charge ratio on the x-axis and relative intensity on the y-axis. The peptide data were searched against the UniprotKB homo sapiens reference proteome using the MS/MS ion search engine. In the above graph, b- ions are numbered from left to right on the N-terminus and y-ions are numbered from right to left on the C- terminus.

B	B Ions	B+2H	B-NH3	B-H2O	AA	Y Ions	Y+2H	Y-NH3	Y-H2O	Y
1	115.1		98.0		N	1,101.5	551.3	1,084.5	1,083.5	9
2	229.1		212.1		N	987.5	494.3	970.5	969.5	8
3	357.2		340.1		Q	873.5	437.2	856.4	855.4	7
4	470.2		453.2		I	745.4	373.2	728.4	727.4	6
5	571.3		554.3	553.3	T	632.3		615.3	614.3	5
6	685.3	343.2	668.3	667.3	N	531.3		514.2		4
7	799.4	400.2	782.3	781.4	N	417.2		400.2		3
8	927.4	464.2	910.4	909.4	Q	303.2		286.2		2
9	1,101.5	551.3	1,084.5	1,083.5	R	175.1		158.1		1

Figure 4.30: *The figure represents fragmentation table of PGK1protein.*

.

The capacity to execute mechanistically different activities has led to the identification of Glyceraldehyde 3 Phosphate protein as a moonlighting protein. It is a glyceraldehyde-3-phosphate dehydrogenase and a nitrosylase, which means it is involved in glycolysis and nuclear processes. With this protein Alzheimer's disease and Huntington's disease are linked to this disease.

Enolase enzymes are cytosolic carbon-oxygen lyases that play an important role in glucose metabolism. Enolase has recently been shown to have a range of regulatory roles other than glycolysis and gluconeogenesis, connected to hypoxia, ischemia, alzheimer.

Pyruvate kinase is glycolysis enzyme that is engaged in the last stage. The phosphate group transfer from phosphoenolpyruvate (PEP) to adenosine diphosphate (ADP), resulting in one pyruvate and one ATP molecule.

Malate Dehydrogenase involves one molecule of pyruvate and one molecule of ATP and appears in many metabolic pathways, including the kreb cycle.

String was used to look at the eight proteins that were dysregulated in AD but not in the control group. To illustrate the degree of evidence for protein connections, MCL clustering was used with the clusters option chosen and the confidence view selected. Enrichment analysis was also

done, and the glucose metabolic process was shown to be the most significantly enriched biological process, with 8 proteins involved.

Interactive association of glucose metabolism with amyloid-beta:

The amyloid beta and fructose bisphosphate aldolase A interaction. Endogenous ligands activated by Amyloid-beta A4 protein; N-APP binds TNFRSF21; Caspase activation and degeneration of both neuronal cell bodies (through caspase-3) and axons (via caspase-6) Fructose-bisphosphate aldolase A plays a critical function in glycolysis and gluconeogenesis. It may also serve as a scaffolding protein (due to its similarities). The fructose-bisphosphate aldolase A belongs to the class I fructose-bisphosphate aldolase family. Their co-expression is zero, however putative homologs are co-expressed in another organism (score 0.063), implying a functional relationship. The results of the experiments and biochemical tests are negligible. The score of association in curated databases is (0.910).

The interaction between ALDOA and LDHB is included in the LDH/MDH superfamily (Lactate Dehydrogenase B). It has been discovered that potential homologs are co-expressed in different species (score 0.113). (score 0.050) were discovered in other creatures interacting. The association score in the curated database is 0. 600, while the combined score is 0.859.

The role of DPD1L modifies sodium current in cardiac; decreased enzymatic activity with increased levels of glycerol 3-phosphate activating the DPD1L-dependent SCN5A phosphorylation pathway with decreased enzymatic activity may even lead to decreased sodium current; cardiac sodium current lessened due to changes in NAD(H) balance caused by the interaction between fructose bisphosphate and DPD1L; In other species, the putative homologs are co-expressed (score 0.081). In other species, the potential homologs were discovered interacting (score 0.054). (with a score of 0.173) in other species, the potential homologs are stated together. The combined score is 0.704.

IDH3A and LDHB interact with one other. Isocitrate dehydrogenase [NAD] alpha subunit mitochondrial; subunit of the enzyme which is catalytic catalyses the decarboxylation of isocitrate (ICT) into alpha-ketoglutarate. Heterodimer consisting of alpha (IDH3A) and beta (IDH3B) subunits have significant basal activity, but the heterotetramer's complete activity (two IDH3A subunits, one IDH3B subunit, and one IDH3G subunit) needs the assembly and

cooperative action of both heterodimers. Lactate dehydrogenase B is a member of the LDH/MDH family of enzymes. The potential homologs are coexpressed in other species (score 0.110). The potential homologs (scoring 0.131) were discovered interacting in different species. In other species, the potential homologs are stated together (score 0.125). The overall grade is 0.536.

PGK1 and IDH3A interact with each other. Although phosphoglycerate kinase 1 is a glycolytic enzyme, it appears that it also functions as a polymerase alpha cofactor protein (primer recognition protein). It's possible that it affects sperm motility. In other genomes, the homologous genes are neighbours (score 0.059). Other species coexpress the potential homologs (score 0.142). In addition, potential homologs in other species are noted together (score 0.209). The overall grade is 0.419.

Interactive association of glucose metabolism with tau:

Tau, a microtubule-associated protein, interacts with actin. Microtubule formation and stability may be important in development and conservation of tau-induced neuronal polarity. In neural plasma membrane components, C-terminus of axonal microtubules binds to the N-terminus implying that tau serves as a linker protein between the two.Polarity at axonal level in body composed of centrosome.It determines TAU/MAPT localization in cells of neurons. The short isoforms make it possible to Short isoforms allow the cytoskeleton to be more flexible. Actincytoplasmic 1 is a protein participates in many forms of cell movement and is found in all eukaryotic cells. Other species coexpress the potential homologs (score 0.062). The potential homologs (scoring 0.157) were discovered interacting in different species. In other species, the potential homologs are stated together (score 0.041). The overall grade is 0.624.

Actin's interaction with fructose bisphosphate aldolase A. Although phosphoglycerate kinase 1 is a glycolytic enzyme, the polymerase alpha cofactor protein. It's possible that it affects sperm motility. The coexpression score is 0.069. Furthermore, potential homologs are found in other species (score 0.146). In other species, the potential homologs were discovered interacting (score 0.087). In addition, potential homologs in other species are noted together (score 0.204). The overall grade is 0.756.

ALDOC and PGK1 interact with one other. The coexpression score is 0.068. Other species coexpress the potential homologs (score 0.177). Other creatures' probable homologs discovered interacting (score 0.098). In addition, potential homologs in other species are noted together (score 0.375). The overall grade is 0.870.

The interaction between PRDX6 and PGK1 increases the decrease of hydrogen peroxide and organic hydroperoxides into water and alcohols, respectively. Thiol-specific peroxidase; peroxiredoxin-6. H2O, as well as organic chains of short, fatty acid, and phospholipid hydroperoxides, can be reduced. It possesses activity of phospholipase and may decrease oxidised sn-2 fatty acyl group of phospholipids (peroxidase activity) or hydrolyze the sn-2 ester bond of phospholipids (phospholipase activity). At acidic pH activities are required for binding to phospholipids at acidic pH and cytosolic pH oxidised phospholipids. The score for coexpression is 0.068. (with a score of 0.114) In other species, the putative homologs are co-expressed. In other species, the potential homologs were discovered interacting (score 0.261). In other species, the potential homologs are stated together (score 0.158). The total score is 0.505. Expressional Analysis of Identified Proteins

Prism is a powerful tool that can do many types of mathematical computations as well as graphical charting, such as curve fitting. The quantity changes from one measurement to the next is described as fold change.The. Ctrl has a fold change of 0.217 in fructose bisphosphate aldolase A when compared to Alzheimer, while AD has a value of 0. 07069.In Alzheimer's disease, its value is lower than normal. Ctrl has a value of 0.18079 when compared to G3P, while it has a value of 0.08665 in AD. Its value is lower in Alzheimer's patients than in healthy people. Enolase has a Ctrl of 0.41299, while AD has a Ctrl of 0.07736. Its value is lower in Alzheimer's patients than in healthy people. The value of pyruvate kinase in AD is 0.07604, while it is 0.3822 in Ctrl. When compared to a healthy brain, its value is lower in Alzheimer's disease. Ctrl is 0.44284 in MDHC and 0.08516 in AD. When compared to AD, it has a lower value. ALDOC is 0.37678 in Ctrl and 0.05164 in AD. It is 0.08289 in Ctrl and 0.16607 in AD. Its value is increase in AD brain tissues as compared to normal brain tissues.

Kinexus Bioinformatics Corporation created phosphonet which is open access to internet resource to support the study of cell signalling systems in academia and industry.

The enzymatic or covalent modification of proteins following protein biosynthesis is called post translational modification.In ALDOA protein the peptide sequence ALAI MEN AN V shows post translational modification.In G3P VFTTMEK,VEG L M TT VHA,ISAP SADA PM,FVMGVNHEK,SNNR VDL M AH, M AS KE.In ENOA DKLIE M DGT,VIGM DVAASE,QANGWGVMVS shows post translational modifications.In ENOA DKLIE M DGT,VIG M DVAASE,QANGWGVMVS.In MDHM SLVDAMNGKE shows post translational modification.

Phosphonet is an open-access, online resource developed by Kinexus Bioinformatics. In academia and industry the corporation to foster the study of cell signalling systems to advance biomedical research.

The bioinformatics analysis of the 34 proteins differentially expressed in proteomic studies .

Identification of Glucose linked protein with Alzheimer

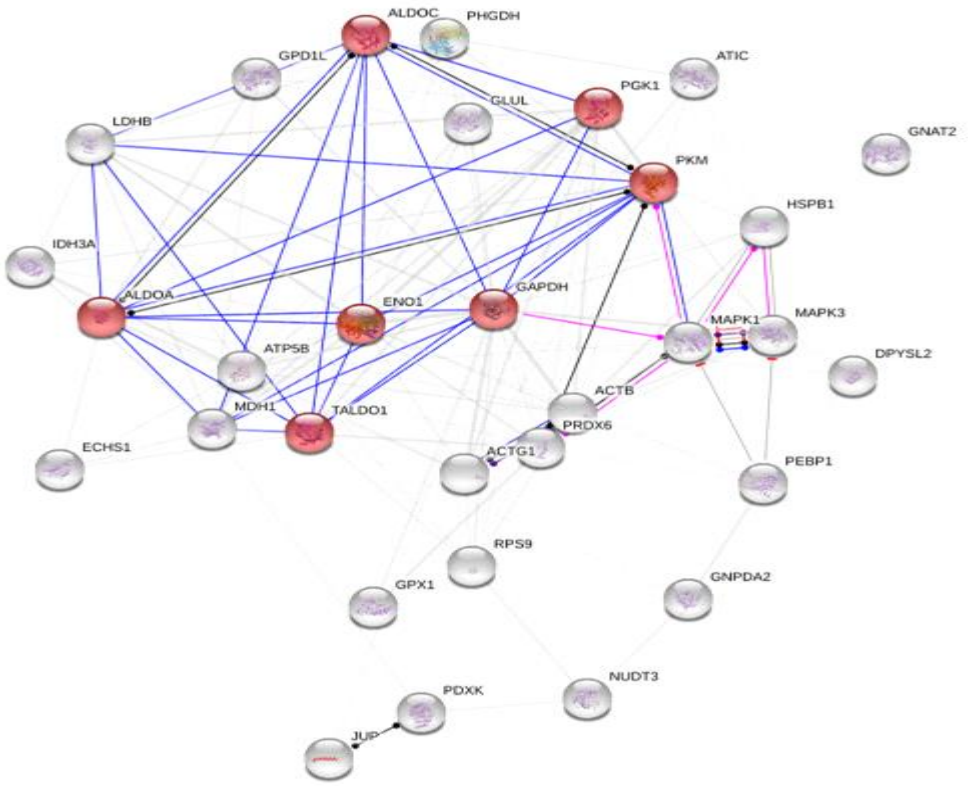

***Figure 4.31**: The proteins involved in glucose metabolism, indicated by the colour red. Eight of these proteins were involved in glucose metabolism linked with Alzheimer.*

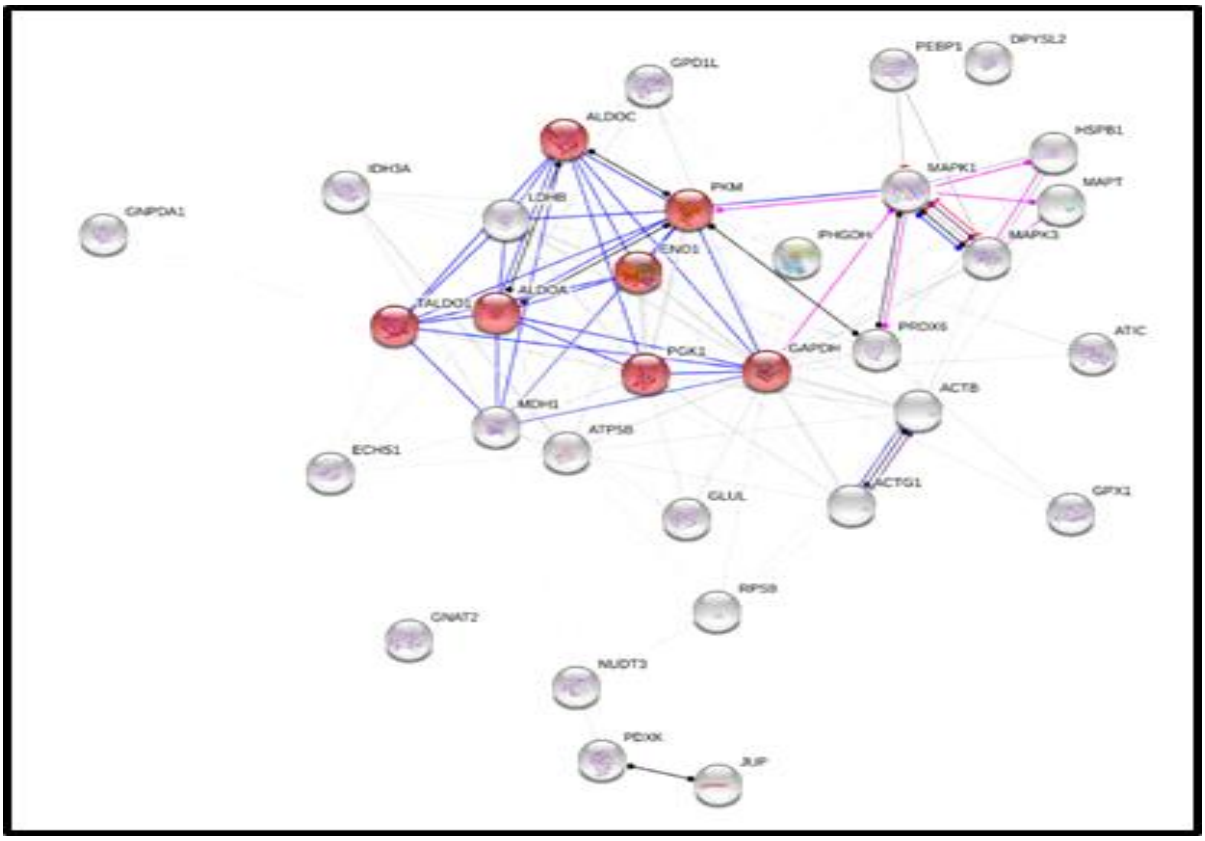

***Figure 4.32**: The plot shows how glucose linked proteins interact with tau*

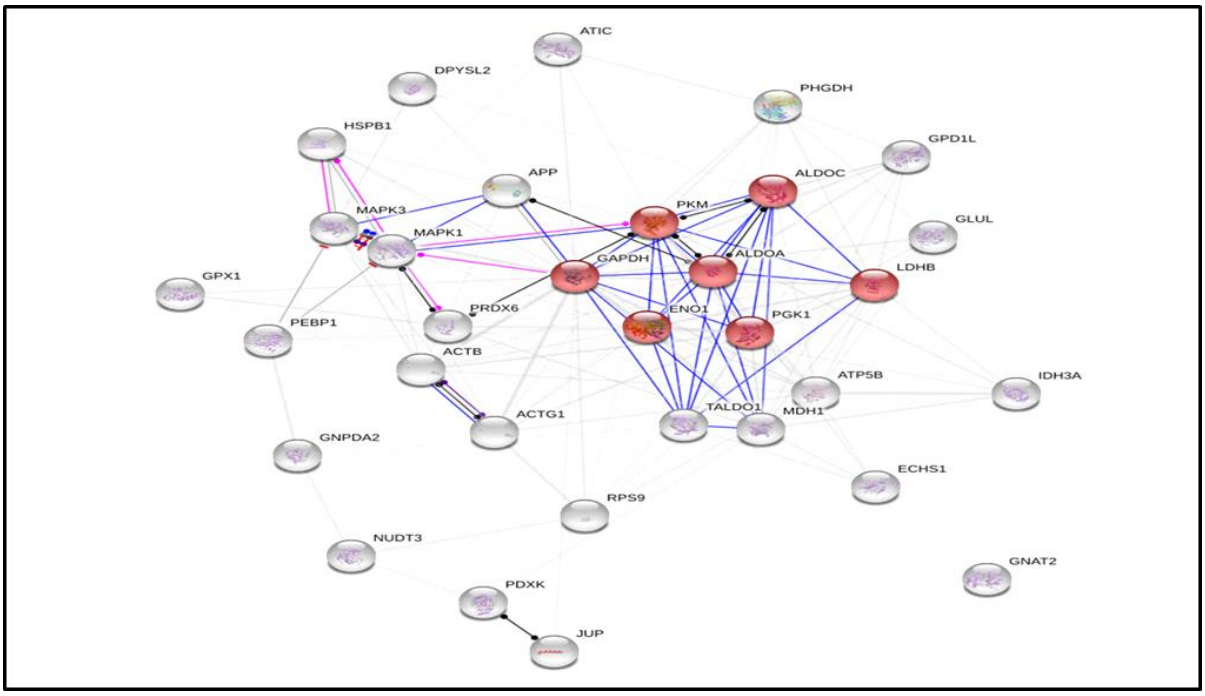

Figure 4.33*:The schematic diagram shows how glucose linked proteins interact with amyloid beta.*

a **b** **c**

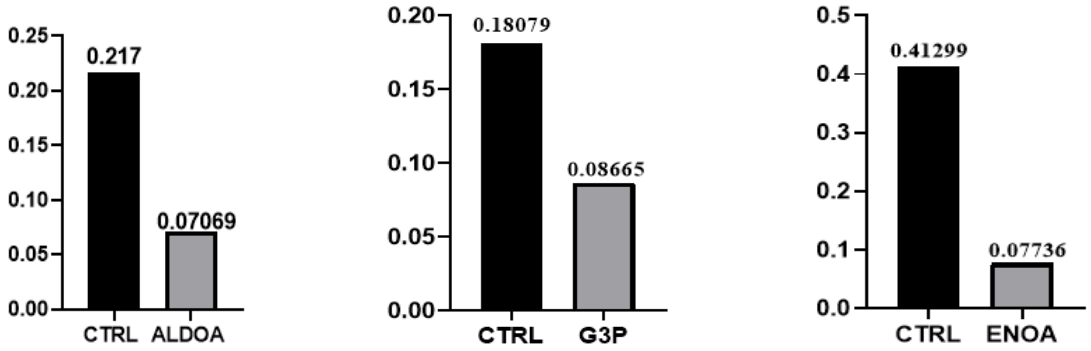

Figure 4.34: (a) Diagram of Fructose Bisphosphate Aldolase A protein fluctuation in Ctrl versus Alzheimer (b) Shows the distribution of Glyceraldehyde 3 Phosphate in Alzheimer compared with Ctrl. (c) Alpha Enolase are shown here in table in Ctrl versus Alzheimer.

a **b** **c**

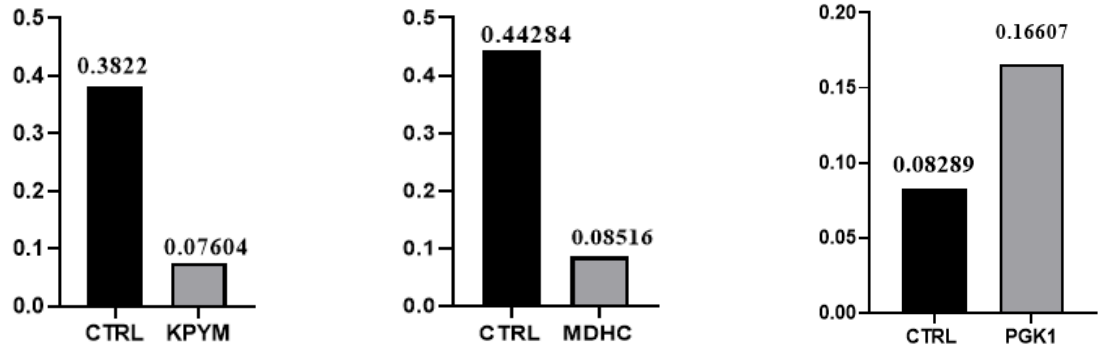

Figure 4.35: (a) The table of Pyruvate kinase protein fluctuation in Ctrl versus Alzheimer (b) Shows the distribution of Malate Dehydrogenase Cytoplasmic in Alzheimer compared with Ctrl. (c) Phosphoglycerate kinase 1 are shown here in table in Ctrl versus Alzheimer.

a **b**

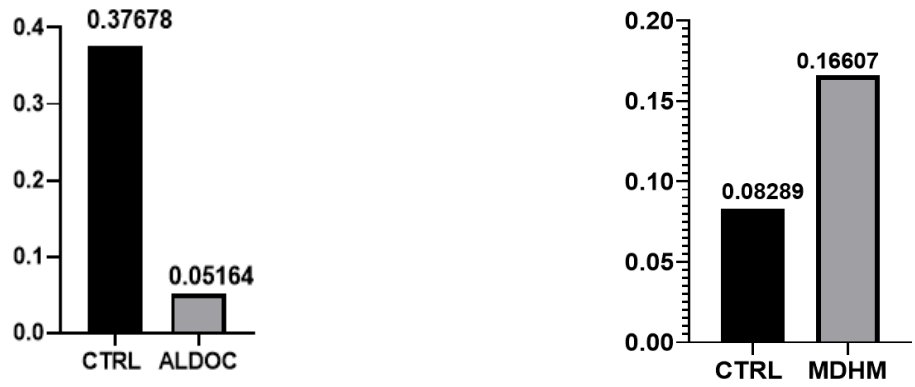

Figure 4.36: (a) The table of Fructose Bisphosphate Aldolase C in Ctrl versus Alzheimer (b) Shows the distribution of Malate Dehydrogenase Mitochondrial in Alzheimer compared with Ctrl.

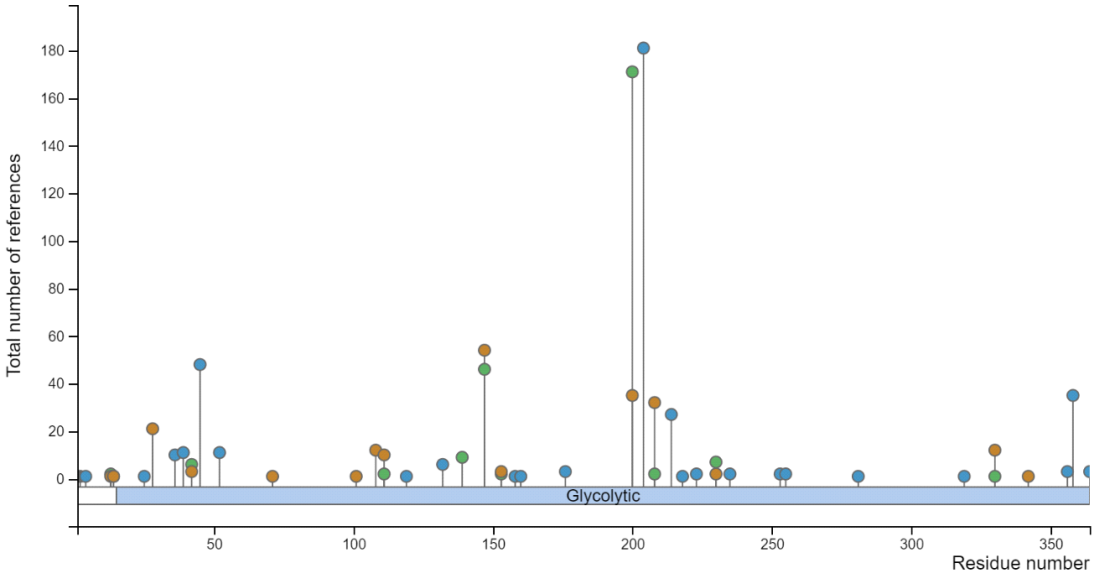

Figure 4.37*: This figure depicts post translational modification of fructose bisphosphate aldolase.*

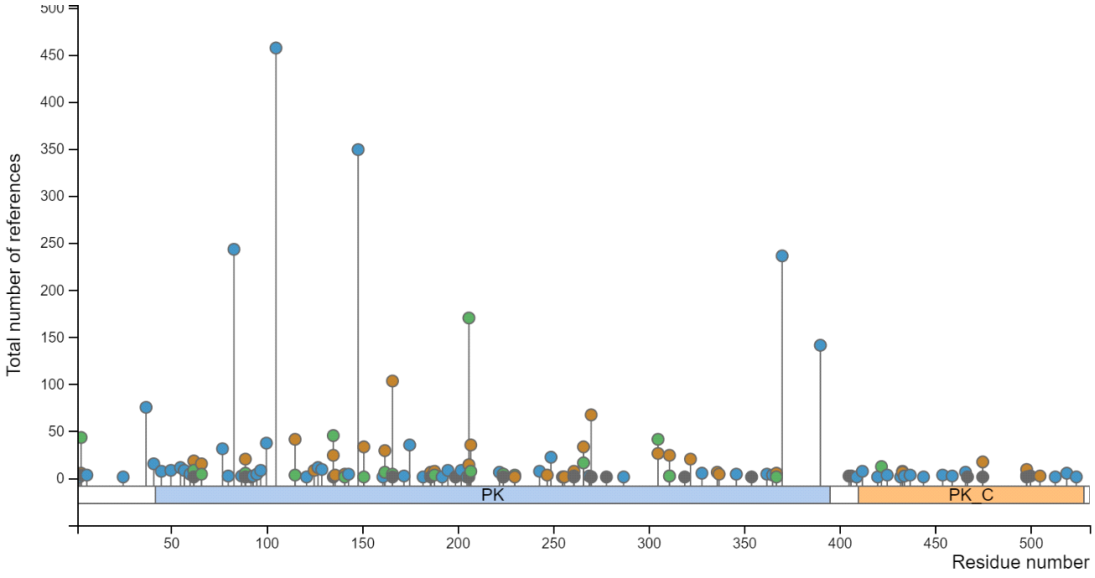

***Figure 4.38**: This figure depicts post translational modification of pyruvate kinase.*

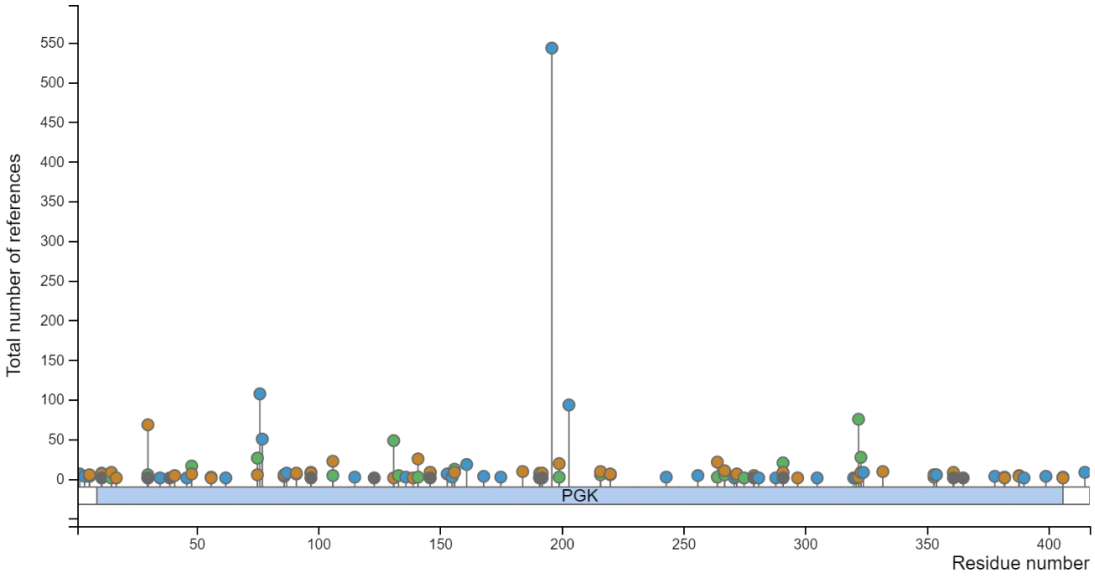

***Figure 4.39**: This figure depicts post translational modification of PGK1*

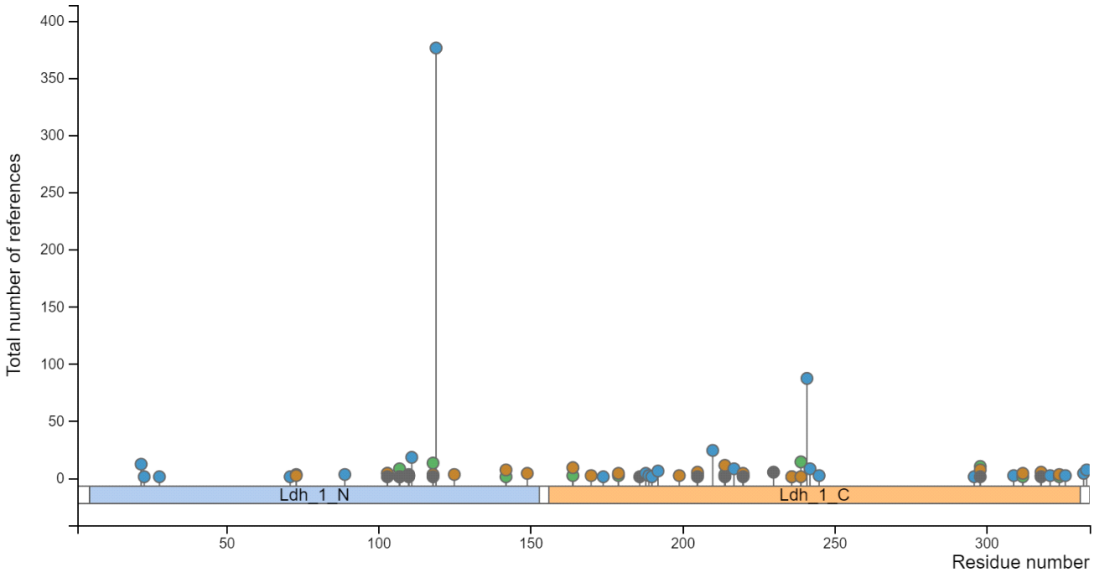

***Figure 4.40**: This figure depicts post translational modification of MDH1*

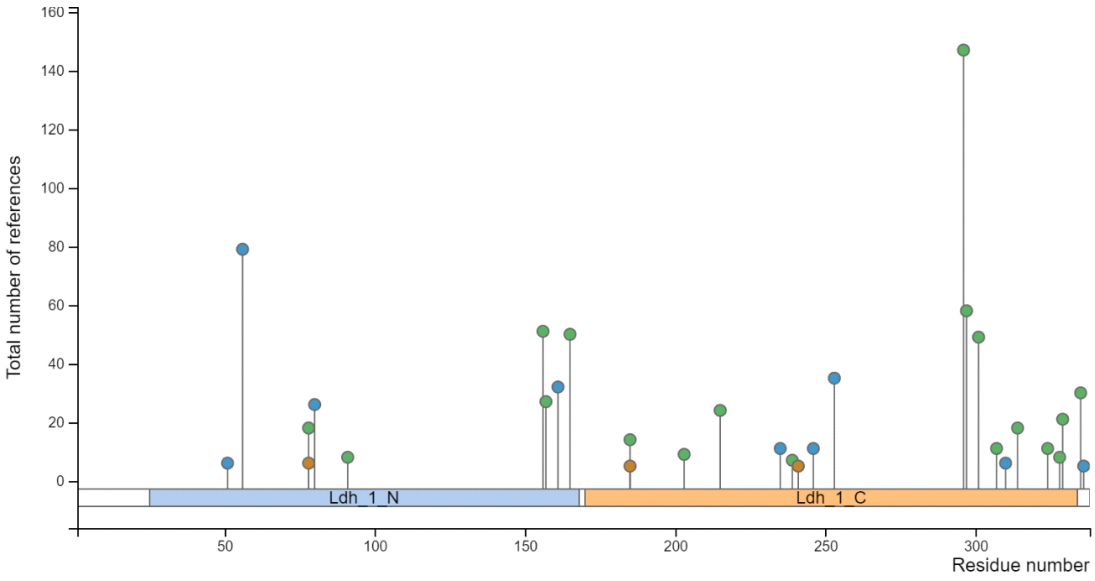

***Figure 4.41**: This figure depicts post translational modification of MDH2.*

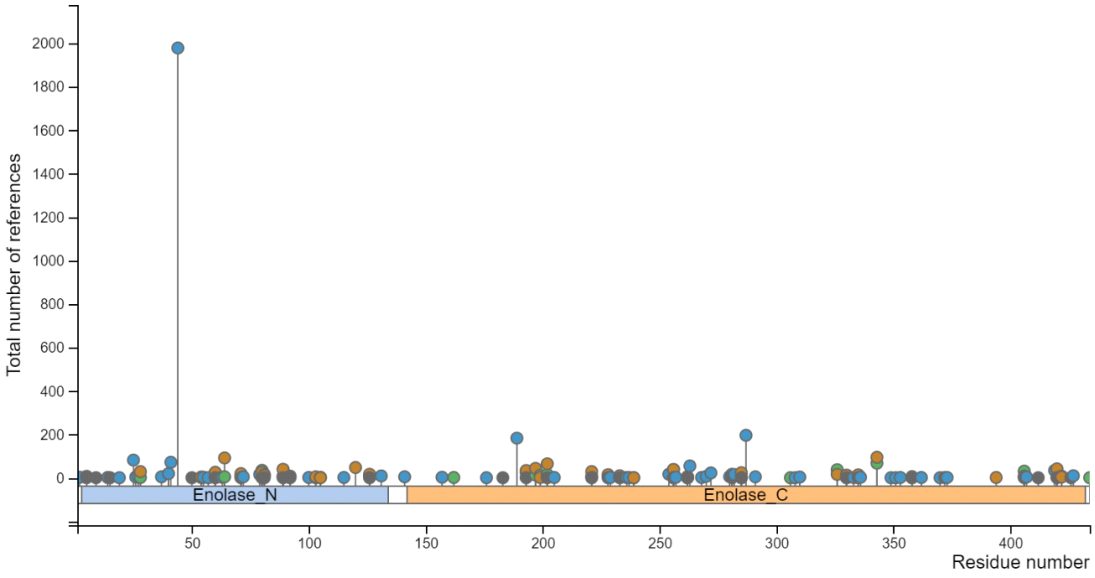

***Figure 4.42**: This figure depicts post translational modification of ENO1.*

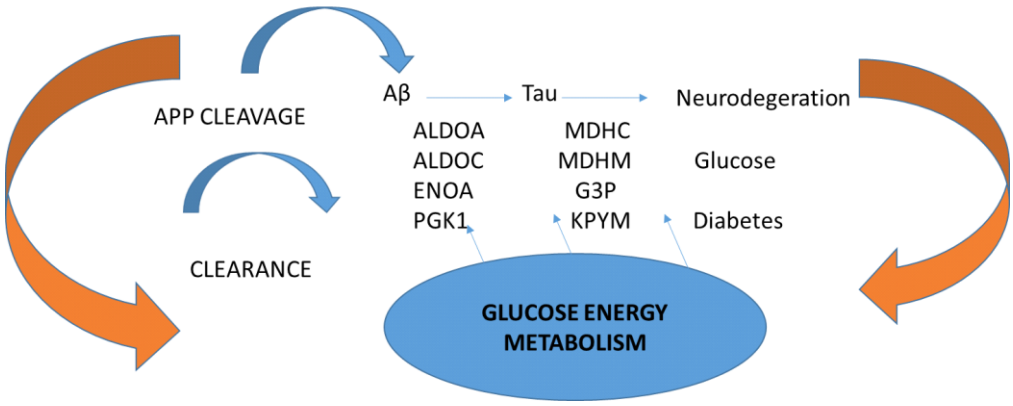

***Figure 4.43**: This figure depicts graphical summary..*

CHAPTER 5 : DISCUSSSION

The prevalent dementia among the aged people, accounts 75%, as a comorbidity or as a separate entity. It is a slow-progressing illness characterized by the emergence of distinctive symptoms in sporadic instances or by a mutation in presenilin 1, 2 or APP. Memory loss and other cognitive impairments obstruct daily living. Alzheimer's disease is responsible for 60–80% of dementia cases. It is characterized by the increase in amyloid-beta (Aβ) plaques or Tau protein tangles in nerve tissue of the brain. The reduction in acetylcholine (ACh) levels is essential factor in development of Alzheimer's disease (Anand et al., 2017).

Early detection of AD is critical since it allows us to seek treatment and plan ahead. AD is correctly diagnosed by examining the patient's medical history and utilizing various imaging therapy methods, such as magnetic resonance imaging (MRI) (MRI). Despite the fact that the actual etiology of the disease is unknown, the pathophysiology of glucose metabolism and this disease is understood. Etiology of AD is complex, involving both genetic predisposition and environmental variables such as increase in tension, heaviness, and abnormal level of lipid, raise risk of dementia around middle age. These chemicals can set off a chain reaction in the neurological system, resulting in neuronal cell death and neuronal malfunction (MohamedKoriem, 2016).

Furthermore, it is important to investigate the history of previously used medicines, drugs, and food. Evoked potentials, which include visual, auditory, brainstem, and somatosensory potentials, also give information on neurofibrillary tangles and tau aggregates (Vlassenko and Raichle, 2015).

Currently, metabolic illness defined as brain's poor use of glucose, as shown by neurodegenerative research over the previous two decades is sporadic type of AD. As a result, Grieb proposed the glucose cascade theory as the cause of sAD. Deficiencies of synthesis of glucose transporters functionality (GLUTs) result from reduced glucose transport: Glucose transporter 1, plays role in transportation of glucose in brain and its absorption into cells of glial, and glucose transporter 3 in neurons uptake glucose. The low metabolic glucose causes hindrance in insulin and death at cellular level. In model animals, glucose intolerance and

memory impairment have been related to excess activation of glycogen synthase kinase-3 (GSK-3), which represent the connection between alterations in glucose turnover and early pathogenic events such as neuroinflammation (Pilipenko et al., 2020). So far, the therapy for Alzheimer's disease is only partially effective, and efforts to create novel therapeutic techniques continue to expand our understanding of the illness's pathogenesis.

Using bioinformatics tools like as String and Scaffold, the current work shows how to characterize glucose related proteins as Alzheimer's disease progresses. Fructose Bisphosphate Aldolase A, Fructose Bisphosphate Aldolase C, Enolase, Glyceraldehyde 3 Phosphate, Pyruvate Kinase, Malate Dehydrogenase Mitochondrial, Phosphoglycerate Kinase 1 are among the proteins discovered. These proteins will help researchers better understand and reveal the relationship between Alzheimer's disease and glucose metabolism, as well as evaluate the function of novel medicines that target the formation of defective glucose metabolism and oxidative stress, which leads to AD.

The primary goal of this research is to identify particular proteins implicated in the connection between faulty glucose metabolism and this disease. This study discovered a group of eight proteins that plays part in this disease, and these proteins were confirmed using bioinformatics methods like String and Scaffold Mass Spectrometry. The variation in glucose metabolism in Alzheimer's patients appears to have a role in the disease's development, according to this study. Protein levels were higher in AD patients matched with controls. Furthermore, subsequent research shows that protein linking between as a neutralising agent may have a potential therapeutic impact. The data was also analysed using string software, and the interaction between the and the protein-ligand was examined. The data was then analysed further using MS/MS spectrometry. Future research into the development and course of this neurological disease will help researchers gain a better grasp of how the disease works.

CHAPTER : 6 REFERENCES

Abolhassani, N., et al. (2017). "Molecular pathophysiology of impaired glucose metabolism, mitochondrial dysfunction, and oxidative DNA damage in Alzheimer's disease brain." Mechanisms of ageing and development **161**: 95-104.

Adams, J. N., et al. (2019). "Relationships between tau and glucose metabolism reflect Alzheimer's disease pathology in cognitively normal older adults." Cerebral Cortex **29**(5): 1997-2009.

Anand, A., et al. (2017). "The present and future of pharmacotherapy of Alzheimer's disease: A comprehensive review." European journal of pharmacology **815**: 364-375.

Bigl, M., et al. (1999). "Activities of key glycolytic enzymes in the brains of patients with Alzheimer's disease." Journal of neural transmission **106**(5-6): 499-511.

Calsolaro, V. and P. Edison (2016). "Alterations in glucose metabolism in Alzheimer's disease." Recent patents on endocrine, metabolic & immune drug discovery **10**(1): 31-39.

Davinelli, S., et al. (2011). "The" Alzheimer's disease signature": potential perspectives for novel biomarkers." Immunity & Ageing **8**(1): 7.

Deshpande, O. A. and S. S. Mohiuddin (2019). Biochemistry, Oxidative Phophorylation. StatPearls [Internet], StatPearls Publishing.

Duran-Aniotz, C. and C. Hetz (2016). "Glucose metabolism: a sweet relief of alzheimer's disease." Current Biology **26**(17): R806-R809.

Grieb, P. (2016). "Intracerebroventricular streptozotocin injections as a model of Alzheimer's disease: in search of a relevant mechanism." Molecular neurobiology **53**(3): 1741-1752.

Huang, L.-K., et al. (2020). "Clinical trials of new drugs for Alzheimer disease." Journal of Biomedical Science **27**(1): 1-13.

Jellinger, K. A. (2020). "Neuropathological assessment of the Alzheimer spectrum." Journal of neural transmission: 1-28.

Kivipelto, M., et al. (2018). "Lifestyle interventions to prevent cognitive impairment, dementia and Alzheimer disease." Nature Reviews Neurology **14**(11): 653-666.

Li, X. b., et al. (2015). "Review of aerobic glycolysis and its key enzymes–new targets for lung cancer therapy." Thoracic cancer **6**(1): 17-24.

Lodish, H., et al. (2000). Electron transport and oxidative phosphorylation. Molecular Cell Biology. 4th edition, WH Freeman.

Mayeux, R. and Y. Stern (2012). "Epidemiology of Alzheimer disease." Cold Spring Harbor perspectives in medicine **2**(8): a006239.

Mosconi, L. (2005). "Brain glucose metabolism in the early and specific diagnosis of Alzheimer's disease." European journal of nuclear medicine and molecular imaging **32**(4): 486-510.

Mosconi, L. (2013). "Glucose metabolism in normal aging and Alzheimer's disease: methodological and physiological considerations for PET studies." Clinical and translational imaging **1**(4): 217-233.

Pilipenko, V., et al. (2020). "Neuroprotective potential of antihyperglycemic drug metformin in streptozocin-induced rat model of sporadic Alzheimer's disease." European journal of pharmacology **881**: 173290.

Reitz, C., et al. (2011). "Epidemiology of Alzheimer disease." Nature Reviews Neurology **7**(3): 137-152.

Reitz, C. and R. Mayeux (2014). "Alzheimer disease: epidemiology, diagnostic criteria, risk factors and biomarkers." Biochemical pharmacology **88**(4): 640-651.

Rotermund, C., et al. (2018). "The therapeutic potential of metformin in neurodegenerative diseases." Frontiers in endocrinology **9**: 400.

Shafiq, M. (2019). Characterization of High-density Prion Protein Oligomers in Rapid Progressive and Sporadic Alzheimer's Disease, Georg-August-Universität Göttingen.

Tang, J., et al. (2019). "Dysfunctional mitochondrial bioenergetics and synaptic degeneration in Alzheimer disease." International Neurourology Journal **23**(Suppl 1): S5.

Vlassenko, A. G. and M. E. Raichle (2015). "Brain aerobic glycolysis functions and Alzheimer's disease." Clinical and translational imaging **3**(1): 27-37.